Circularly polarized few-cycle optical rogue waves: Rotating reduced Maxwell-Bloch equations

Shuwei Xu,[1,2] K. Porsezian,[3] Jingsong He,[4,*] and Yi Cheng[1]
[1]*School of Mathematical Sciences, USTC, Hefei, Anhui 230026, P. R. China*
[2]*Beijing Computational Science Research Center, Beijing 100084, P. R. China*
[3]*Department of Physics, Pondicherry University, Puducherry 605014, India*
[4]*Department of Mathematics, Ningbo University, Ningbo, Zhejiang 315211, P. R. China*
(Received 12 August 2013; published 27 December 2013)

The rotating reduced Maxwell-Bloch (RMB) equations, which describe the propagation of few-cycle optical pulses in a transparent media with two isotropic polarized electronic field components, are derived from a system of complete Maxwell-Bloch equations without using the slowly varying envelope approximations. Two hierarchies of the obtained rational solutions, including rogue waves, which are also called few-cycle optical rogue waves, of the rotating RMB equations are constructed explicitly through degenerate Darboux transformation. In addition to the above, the dynamical evolution of the first-, second-, and third-order few-cycle optical rogue waves are constructed with different patterns. For an electric field E in the three lower-order rogue waves, we find that rogue waves correspond to localized large amplitude oscillations of the polarized electric fields. Further a complementary relationship of two electric field components of rogue waves is discussed in terms of analytical formulas as well as numerical figures.

DOI: 10.1103/PhysRevE.88.062925 PACS number(s): 42.81.Dp, 42.65.Tg, 42.65.Re, 02.30.Ik

I. INTRODUCTION

Ultrashort optical pulses are widely used in many fields which include testing ultrahigh speed semiconductor devices, precise processing of materials, triggering and tracing chemical reactions, wavelength division multiplexing, and many branches of strong-field physics [1,2]. Because of the tremendous progress made in the area of laser technology, pulses having few cyclic oscillations in the electric and magnetic fields have been generated in laboratory [1,2]. Furthermore, more intense and shorter pulses, even a single-cycle pulse, have been reported recently [3,4]. These remarkable inventions are responsible for real-time observation and steering of electronic dynamics on the atomic scale [2]. It is obviously impossible to use the concept of an envelope to model the propagation of a few-cycle ultrashort pulse. Thus, a challenging problem in the study of ultrashort pulses is that the widely used slowly varying envelope approximation (SVEA) is no longer valid in the case of short pulses [5–8]. Naturally, two kinds of models, improved SVEA and non-SVEA models, associated with the ultrashort pulses have been well studied in Refs. [9–11]. On one hand, several attempts have been made to improve the SVEA and show their efficiency, see, e.g., Refs. [12,13]. On the other hand, non-SVEA models have been equally studied intensively, see, e.g., Refs. [14–21]; also, one can find more comprehensive examples in two survey papers [10,11].

It is a well-known fact that the reduced Maxwell-Bloch (RMB) equations [22–24] have been derived to model self-induced transparency (SIT) phenomenon [25–27] without using the so called SVEA method from the mid 1970s [28–31]. Although such derivation has attracted a lot of interest among researchers, the generalization of the RMB equations is of current research interest due to rapid developments and application of the ultrashort pulses [32–34]. Recently, Steudel and Zabolotskii have constructed the RMB equations for circularly polarized light with two isotropic electronic field components, which are called rotating RMB equations of the form [35]

$$
\begin{aligned}
(c\partial_z+\partial_t)\varepsilon_x &= -2\pi d n \partial_t R_x,\\
(c\partial_z+\partial_t)\varepsilon_y &= -2\pi d n \partial_t R_y,\\
\partial_t R_x &= -\omega_0 R_y - \frac{2d}{\hbar}\varepsilon_y R_z,\\
\partial_t R_y &= \omega_0 R_y + \frac{2d}{\hbar}\varepsilon_x R_z,\\
\partial_t R_z &= \frac{2d}{\hbar}(R_x\varepsilon_y - R_y\varepsilon_x).
\end{aligned} \tag{1}
$$

Here, ε_x and ε_y are the electric field components, and (R_x,R_y,R_z) is the Bloch vector. c is the velocity of light in vacuum, d is the dipole moment, ω_0 is a common resonance frequency, $\hbar$ is the Planck constant, and n denotes the number density of atoms. Using the following transformations

$$
\begin{aligned}
\chi &= \frac{4\pi d^2 n}{\hbar c}z, \quad \tau = \omega_0\left(t-\frac{z}{c}\right),\\
E_{x,y} &= \frac{2d}{\hbar\omega_0}\varepsilon_{x,y}, \quad E = E_x + iE_y,\\
R &= R_x + iR_y, \quad R^z = R_z,
\end{aligned} \tag{2}
$$

Eq. (1) can be rewritten in the following form [35]:

$$
\begin{aligned}
R_\tau &= i(R+ER^z), \quad S_\tau = -i(S+FR^z),\\
R^z{}_\tau &= \frac{i}{2}(RF-SE), \quad E_\chi = -R_\tau, \quad F_\chi = -S_\tau,
\end{aligned} \tag{3}
$$

with the condition $F=E^*$ and $S=R^*$. Here, E and R represent complex field envelopes, R^z is a real variable, and asterisk denotes complex conjugation. It is worth noting that rotating RMB equations is an integrable system that admits the Kaup-Newell-type spectral problem [36] with the

*hejingsong@nbu.edu.cn, jshe@ustc.edu.cn

compatibility condition

$$U_\chi - V_\tau + [U,V] = 0 \tag{4}$$

of the following linear spectral problem [35]:

$$\partial_\tau \psi = U\psi = \frac{1}{2}(J\xi^2 + U_1\xi)\psi, \tag{5}$$

$$\partial_\chi \psi = V\psi = -\frac{\xi}{2(1+\xi^2)}(-JR^z\xi + V_0)\psi, \tag{6}$$

with

$$J = \begin{pmatrix} -i & 0 \\ 0 & i \end{pmatrix}, \quad U_1 = \begin{pmatrix} 0 & E \\ F & 0 \end{pmatrix},$$
$$V_0 = \begin{pmatrix} 0 & R \\ S & 0 \end{pmatrix}, \quad \psi = \begin{pmatrix} \psi_1 \\ \psi_2 \end{pmatrix}.$$

Here, ξ is an eigen value parameter. Later, the rotating RMB equations with anisotropy have been derived [37–39], and the solutions of rotating RMB equations with and without anisotropy were constructed using Bäcklund transformation and inverse scattering method. Note that the differences between rotating RMB equations with and without isotropy [35,37] depends on the relationship between the dipole moments d_x and d_y. The paper mainly considered the rotating RMB equations with the dipole moment condition $d_x = d_y$. On the basis of detailed explanation of the RMB equations from the idea of the physical relevance of ultrashort optical pulses, several integrable models of a few cycle pulses associated with the extensions of the RMB equations were also reported in Refs. [32–34].

Our recent results regarding the rogue waves [40,41] of nonlinear Schrödinger (NLS) equation coupled with Maxwell-Bloch (MB) equation and the Hirota equation coupled with MB equation motivate us to study the possibilities of rogue waves in the rotating RMB [35] equations. Rogue waves have not only been reported in the investigation of oceanic conditions [42–44] but also in photonic crystal fibers [45,46], etc. One of the widely accepted prototypes of rogue waves in one-dimensional space and time is the Peregrine soliton [47] derived from the NLS equation, which is usually in the form of a single dominant peak accompanied by one deep cave at each side in a plane with a nonzero boundary. Recently, by applying Darboux transformation (DT) method [48–51], different patterns of the rogue waves for NLS and the derivative nonlinear Schrödinger (DNLS) equations have been reported in Refs. [52–59]. Therefore, the purpose of this paper is twofold. First, we attempt to find rogue waves of Eq. (3) [35] as a model of few-cycle optical pulse propagation. These rogue wave solutions may be useful to generate ultraintense optical pulses because of its very large amplitude and ultrabroad frequency spectrum. Second, it aims at identifying differences and similarities between the two circularly polarized electric field components $\varepsilon_{x,y}$. For simplicity, we study their equivalent counterparts $E_{x,y}$ in Eq. (2) with the help of rogue wave solutions. The second result will show a main difference between a circularly polarized wave and a plane polarized wave that has not been discussed in Ref. [35].

In order to derive rogue waves, we need to consider the rational solutions of the rotating RMB equations [35]. These equations are integrable systems that admit the Kaup-Newell spectral problem [36]. We must notice that Steudel and Zabolotskii first have given some nondegenerate solutions, such as the breather solution corresponding to the 2π-pulse of self-induced transparency in terms of Vandermonde-like determinants by using n-fold Bäcklund transformation. However, unlike the usual Bäcklund transformation, they used solutions of Riccati equations for the quotient $\beta = \psi_2/\psi_1$ (see Eqs. (12) and (13) in Ref. [35]), which fails to generate the degenerate higher-order Bäcklund transformation if the component ψ_1 of eigenfunction ψ of the Kaup-Newell spectral problem has a zero point. However, as we have discussed in Ref. [57], it is necessary to set ξ_0 (which will be defined explicitly later) to be a zero point of the eigenfunction ψ in order to generate rogue waves by means of the degenerate Darboux (or Bäcklund) transformation. So we shall construct the determinant representation of the n-fold DT and formulas of $E^{[n]}$, $F^{[n]}$, $R^{[n]}$, $S^{[n]}$, and $R^{z[n]}$ by eigenfunctions ψ of spectral problem. Furthermore, two kinds of rational solutions, including rational solitons and rogue waves, of the rotating RMB equations are given by the degenerate DT from the vacuum and monochromatic wave. By taking advantage of a simpler form of the first-order rational soliton, we can construct a two-peak rational soliton of R and a criterion of its existence. We also shall construct the higher-order rogue waves of the rotating RMB equations and then use it to discuss the relationship between two electric field components E_x and E_y.

The structure of this paper is arranged as follows: In Sec. II, we provide the expressions of the $E^{[n]}$, $R^{[n]}$, and ${R_z}^{[n]}$ of the rotating RMB equations by using n-fold DT. In Sec. III, we present the nth-order rational solutions of the rotating RMB equations from the vacuum and monochromatic wave through degenerate DT and discuss its properties for the rational solutions. Finally, we summarize our results in Sec. IV.

II. DARBOUX TRANSFORMATION

In the following, onefold DT of the unreduced linear problem Eqs. (5) and (6) is defined as a 2×2 matrix transformation in terms of ψ, U, and V,

$$\psi^{[1]} = T\psi, \quad U^{[1]} = (T_\tau + TU)T^{-1},$$
$$V^{[1]} = (T_\chi + TV)T^{-1}, \tag{7}$$

to retain the Lax pair, i.e.,

$$\psi^{[1]}{}_\tau = U^{[1]}\psi^{[1]}, \quad \psi^{[1]}{}_\chi = V^{[1]}\psi^{[1]}. \tag{8}$$

At the same time, the old potential (or seed solution)(E, F, R, S, R^z) in spectral matrices U, V are mapped into new potentials (or new solution) ($E^{[1]}$, $F^{[1]}$, $R^{[1]}$, $S^{[1]}$, $R^{z[1]}$) in terms of transformed spectral matrixes $U^{[1]}$, $V^{[1]}$. Considering the application of the representation for the n-fold DT by means of the determinant of unreduced linear problem Eqs. (5) and (6) with different eigenvalues in the following context, we need to introduce n eigenfunctions ψ_k associated with ξ_k as

$$\psi_k = \psi_k(\xi_k) = \begin{pmatrix} \psi_{k1} \\ \psi_{k2} \end{pmatrix}, \quad k = 1,2,\ldots,n,$$
$$\psi_{k1} = \psi_{k1}(\tau,\chi,\xi_k), \quad \psi_{k2} = \psi_{k2}(\tau,\chi,\xi_k). \tag{9}$$

A. Onefold Darboux transformation

Without loss of generality, let the Darboux matrix T be defined in the form [35]

$$T_1 = T_1(\xi;\xi_1) = \begin{pmatrix} a_1 & 0 \\ 0 & d_1 \end{pmatrix}\xi + \begin{pmatrix} 0 & b_0 \\ c_0 & 0 \end{pmatrix}. \tag{10}$$

Here, a_1,d_1 are undetermined function of (τ,χ), which will be parametrized by the eigenfunction ψ_1 associated with ξ_1 and seed (E, F, R, S, R^z) in the spectral problem. Note that b_0 and c_0 are constants from the coefficients of ξ^0 in Eqs. (A3) and (A5), which are given in Appendix A.

Theorem 1. The elements of onefold DT are parametrized by the eigenfunction ψ_1 associated with ξ_1 as

$$d_1 = \frac{1}{a_1}, \quad a_1 = -\frac{\psi_{12}}{\psi_{11}}, \quad b_0 = c_0 = \xi_1, \tag{11}$$

then

$$T_1(\xi;\xi_1) = \begin{pmatrix} -\xi\frac{\psi_{12}}{\psi_{11}} & \xi_1 \\ \xi_1 & -\xi\frac{\psi_{11}}{\psi_{12}} \end{pmatrix}. \tag{12}$$

T_1 implies the following new solutions

$$\begin{aligned} E^{[1]} &= E\frac{a_1}{d_1} + \frac{2ib_0}{d_1}, \\ F^{[1]} &= F\frac{d_1}{a_1} - \frac{2ic_0}{a_1}, \\ R^{z[1]} &= R^z + \frac{2ia_{1\chi}}{a_1}, \\ R^{[1]} &= -\frac{2b_{0\chi}}{d_1} + R\frac{a_1}{d_1} - 2iR^z\frac{b_0}{d_1} + 2a_{1\chi}b_0, \\ S^{[1]} &= -\frac{2c_{0\chi}}{a_1} + S\frac{d_1}{a_1} + 2iR^z\frac{c_0}{a_1} + 2d_{1\chi}c_0, \end{aligned} \tag{13}$$

and the corresponding new eigenfunction associated with ξ_k is

$$\psi_k^{[1]} = \begin{pmatrix} \frac{1}{\psi_{11}}\begin{vmatrix} -\xi_k\psi_{k1} & \psi_{k2} \\ -\xi_1\psi_{11} & \psi_{12} \end{vmatrix} \\ \frac{1}{\psi_{12}}\begin{vmatrix} -\xi_k\psi_{k2} & \psi_{k1} \\ -\xi_1\psi_{12} & \psi_{11} \end{vmatrix} \end{pmatrix}. \tag{14}$$

Proof. We need to parametrize T_1 by the eigenfunctions associated with ξ_1. This can be realized through a system of equations defined by its kernel, i.e., $T_1(\xi)|_{\xi=\xi_1}\psi_1 = 0$. Solving this system of algebraic equations for (a_1,d_1,b_0,c_0), Eq. (11) is obtained. Next, substituting (a_1,d_1,b_0,c_0) into the equations from the coefficients of ξ^2 in Eqs. (A3) and (A5), new solutions $E^{[1]}$, $F^{[1]}$, $R^{[1]}$, $S^{[1]}$, and $R^{z[1]}$ are given as in Eq. (13). Further, by using explicit matrix representation Eq. (12) of T_1, the new eigenfunction takes the form $\psi_j^{[1]} = T_1(\xi;\xi_1)|_{\xi=\xi_j}\psi_j$ for $j \geqslant 2$. ■

It is trivial to confirm that $\psi_1^{[1]} = 0$ by making use of T_1 in Eq. (12) or by the representation of transformed eigenfunction in Eq. (14).

B. *n*-fold Darboux transformation

The main result in this subsection is the determinant representation of the n-fold DT for unreduced rotating RMB equations. According to the form of T_1 in Eq. (10), the n-fold DT is assumed to be in the form [35] of

$$T_n = T_n(\xi;\xi_1,\xi_2,\ldots,\xi_n) = \sum_{k=0}^{n} P_k\xi^{n-k}, \tag{15}$$

with

$$\begin{aligned} P_{2l} &= \begin{pmatrix} a_{2l} & 0 \\ 0 & d_{2l} \end{pmatrix}, \quad P_{2l-1} = \begin{pmatrix} 0 & b_{2l-1} \\ c_{2l-1} & 0 \end{pmatrix}, \\ P_n &= \begin{pmatrix} \xi_1\xi_2\ldots\xi_n & 0 \\ 0 & \xi_1\xi_2\ldots\xi_n \end{pmatrix} \quad (\text{if } n \text{ is even}), \\ P_n &= \begin{pmatrix} 0 & \xi_1\xi_2\ldots\xi_n \\ \xi_1\xi_2\ldots\xi_n & 0 \end{pmatrix} \quad (\text{if } n \text{ is odd}). \end{aligned}$$

Here, P_n is a constant matrix, P_i is the function of τ and χ. In particular, if n is even or odd, P_n leads to the separate discussion on the determinant representation of T_n in the following by means of its kernel. Specifically, from algebraic equations,

$$\begin{aligned} &\psi_l^{[n]} = T_n(\xi;\xi_1,\xi_2,\ldots,\xi_n)|_{\xi=\xi_l}\psi_l = \sum_{k=0}^{n} P_k\xi_l^{n-k}\psi_l = 0, \\ &l = 1,2,\ldots,n, \end{aligned} \tag{16}$$

the coefficients of P_i are solved by Cramer's rule. The resulting determinant representation of the T_n is given in Appendix B.

Theorem 2. Starting from a seed (E, F, R, S, R^z), the n-fold DT T_n defined by Appendix B generates the following new solutions ($E^{[n]}$, $F^{[n]}$, $R^{[n]}$, $S^{[n]}$, and $R^{z[n]}$).

$$\begin{aligned} E^{[n]} &= E\frac{a_0}{d_0} + \frac{2i\,b_1}{d_0}, \quad F^{[n]} = F\frac{d_0}{a_0} - \frac{2\,i\,c_1}{a_0} \\ R^{z[n]} &= R^z + \frac{2ia_{0\chi}}{a_0}, \\ R^{[n]} &= -\frac{2b_{1\chi}}{d_0} + R\frac{a_0}{d_0} - iR^z\left(\frac{b_1}{d_0} + a_0b_1\right) + 2a_{0\chi}b_1, \\ S^{[n]} &= -\frac{2c_{1\chi}}{a_0} + S\frac{d_0}{a_0} + iR^z\left(\frac{c_1}{a_0} + d_0c_1\right) + 2d_{0\chi}c_1. \end{aligned} \tag{17}$$

Proof. We consider the transformed new solutions ($E^{[n]}$, $F^{[n]}$, $R^{[n]}$, $S^{[n]}$, and $R^{z[n]}$) of unreduced RMB equations corresponding to the n-fold DT. Under covariant requirement of spectral problem, the transformed form of spectral problem should be

$$\partial_\tau\psi^{[n]} = U^{[n]}\psi = \frac{1}{2}\left(J\xi^2 + U_1^{[n]}\xi\right)\psi, \tag{18}$$

$$\partial_\chi\psi^{[n]} = V^{[n]}\psi = -\frac{\xi}{2(1+\xi^2)}\left(-JR^{z[n]}\xi + V_0^{[n]}\right)\psi, \tag{19}$$

with

$$U_1 = \begin{pmatrix} 0 & E^{[n]} \\ F^{[n]} & 0 \end{pmatrix}, \quad V_0 = \begin{pmatrix} 0 & R^{[n]} \\ S^{[n]} & 0 \end{pmatrix}, \quad \psi = \begin{pmatrix} \psi_1 \\ \psi_2 \end{pmatrix},$$

and then satisfy the following equation on τ-part

$$T_{n\tau} + T_n U = U^{[n]} T_n. \tag{20}$$

Substituting T_n given by Eq. (15) into Eq. (20), and then comparing the coefficients of ξ^{n+1}, it yields

$$\begin{aligned} E^{[n]} &= E\frac{a_0}{d_0} + \frac{2ib_1}{d_0},\\ F^{[n]} &= F\frac{d_0}{a_0} - \frac{2ic_1}{a_0}. \end{aligned} \tag{21}$$

Similarly, from the equation of χ-part

$$T_{n\chi} + T_n V = V^{[n]} T_n, \tag{22}$$

and then comparing the coefficients of ξ^{n+2} and ξ^{n+1}, we get

$$\begin{aligned} R^{z[n]} &= R^z + \frac{2ia_{0\chi}}{a_0},\\ R^{[n]} &= -\frac{2b_{1\chi}}{d_0} + R\frac{a_0}{d_0} - iR^z\left(\frac{b_1}{d_0} + a_0 b_1\right) + 2a_{0\chi} b_1,\\ S^{[n]} &= -\frac{2c_{1\chi}}{a_0} + S\frac{d_0}{a_0} + iR^z\left(\frac{c_1}{a_0} + d_0 c_1\right) + 2d_{0\chi} c_1. \end{aligned} \tag{23}$$

Furthermore, substituting a_0, d_0, b_1, c_1 from Eq. (B2) ($n = 2k$) and from Eq. (B4) ($n = 2k+1$) into Eqs. (21) and (23), we get the final form of new solutions ($E^{[n]}$, $F^{[n]}$, $R^{[n]}$, $S^{[n]}$, and $R^{z[n]}$). ■

Here, $R^{z[n]}$, $R^{[n]}$, and $S^{[n]}$ are the expressions obtained in terms of $n \times n$ determinant of eigenfunctions (a_0, d_0, b_1, c_1), but which are expressed by $(n+1) \times (n+1)$ determinants in Ref. [35]. Moreover, we use eigenfunctions ψ_j to construct determinants in n-fold DT instead of quotient $\beta_j = \psi_{j2}/\psi_{j1}$ of two components as reported in Ref. [35].

C. Reduction of the Darboux transformation

Under the reduction conditions $F = E^*$, $S = R^*$, R^z is real, the eigenfunction $\psi_k = \binom{\psi_{k1}}{\psi_{k2}}$ associated with eigenvalue ξ_k has the following relationship [35]:

(i) $\psi_{k1}^* = \psi_{k2}$, $\xi_k = \xi_k{}^*$;

(ii) $\psi_{k1}{}^* = \psi_{l2}$, $\psi_{k2}{}^* = \psi_{l1}$, $\xi_k{}^* = \xi_l$, where $k \neq l$.

According to this property of the eigenfunctions, and setting $n = 2k$ and $l = 1,3,\ldots,2k-1$, and if we now choose k distinct eigenvalues and eigenfunctions in n-fold DTs as

$$\begin{aligned} &\xi_l \leftrightarrow \psi_l = \begin{pmatrix}\psi_{l1}\\ \psi_{l2}\end{pmatrix}, \quad \text{and}\\ &\xi_{2j} = \xi_{2j-1}^* \leftrightarrow \psi_{2j} = \begin{pmatrix}\psi_{2j-1\,2}^*\\ \psi_{2j-1\,1}^*\end{pmatrix},\\ &j = 1,2,3,\ldots,k, \end{aligned} \tag{24}$$

we finally find that reduction conditions hold good, i.e., $F^{[n]} = (E^{[n]})^*$, $S^{[n]} = (R^{[n]})^*$, and $R^{z[n]}$ is real. With the help of choice in Eq. (24), T_n is the n-fold DT of the rotating RMB equations, and thus Theorem 2 provides new solutions of them. Similarly, for $n = 2k+1$, we can also find suitable generating functions to obtain the reduction of n-fold DT.

III. THE TWO HIERARCHY OF RATIONAL SOLUTIONS

In this section, we shall present explicit solutions of the rotating RMB equations through DT by using Eq. (24). Thus, it is easy to check that

$$W_n = (-1)^{\frac{n}{2}} \widetilde{W_n}^*, \quad \delta_{n1} = (-1)^{\frac{n}{2}} \delta_{n2}^*$$

in Appendix B. Taking Eq. (B2) ($n = 2k$) into Eqs. (21) and (23), these solutions become

$$\begin{aligned} E^{[k]} &= Ea_0^2 + 2ib_1 a_0,\\ R^{[k]} &= -2b_{1\chi} a_0 + Ra_0^2 - 2iR^z b_1 a_0 + 2a_{0\chi} b_1,\\ R^{z[k]} &= R^z + \frac{2ia_{0\chi}}{a_0}, \end{aligned} \tag{25}$$

with

$$a_0 = \frac{H_{n1}{}^*(-1)^{\frac{n}{2}}}{H_{n1}}, \quad b_1 = -\frac{H_{n2}}{H_{n1}},$$

$$H_{n1} = \begin{vmatrix} \xi_1^{n-1}\psi_{11} & \xi_1^{n-2}\psi_{12} & \ldots & \xi_1\psi_{11} & \psi_{12}\\ \xi_1^{*n-1}\psi_{12}^* & \xi_1^{*n-2}\psi_{11}^* & \ldots & \xi_1^*\psi_{12}^* & \psi_{11}^*\\ \vdots & \vdots & \vdots & \vdots & \vdots\\ \xi_{n-1}^{n-1}\psi_{n-11} & \xi_{n-1}^{n-2}\psi_{n-12} & \ldots & \xi_{n-1}\psi_{n-11} & \psi_{n-12}\\ \xi_{n-1}^{*\ n-1}\psi_{n-12}^* & \xi_{n-1}^{*\ n-2}\psi_{n-11}^* & \ldots & \xi_{n-1}^*\psi_{n-12}^* & \psi_{n-11}^* \end{vmatrix}, \tag{26}$$

$$H_{n2} = \begin{vmatrix} \xi_1^{n}\psi_{11} & \xi_1^{n-2}\psi_{11} & \ldots & \xi_1\psi_{12} & \psi_{11}\\ \xi_1^{*n}\psi_{12}^* & \xi_1^{*n-2}\psi_{12}^* & \ldots & \xi_1^*\psi_{11}^* & \psi_{12}^*\\ \vdots & \vdots & \vdots & \vdots & \vdots\\ \xi_{n-1}^{n}\psi_{n-11} & \xi_{n-1}^{n-2}\psi_{n-11} & \ldots & \xi_{n-1}\psi_{n-12} & \psi_{n-11}\\ \xi_{n-1}^{*\ n}\psi_{n-12}^* & \xi_{n-1}^{*\ n-2}\psi_{n-12}^* & \ldots & \xi_{n-1}^*\psi_{n-11}^* & \psi_{n-12}^* \end{vmatrix}.$$

In order to get the rational solutions, we only need to seek the eigenvalue degeneration of $\frac{H_{n1}^*}{H_{n1}}$ and $\frac{H_{n2}}{H_{n1}}$.

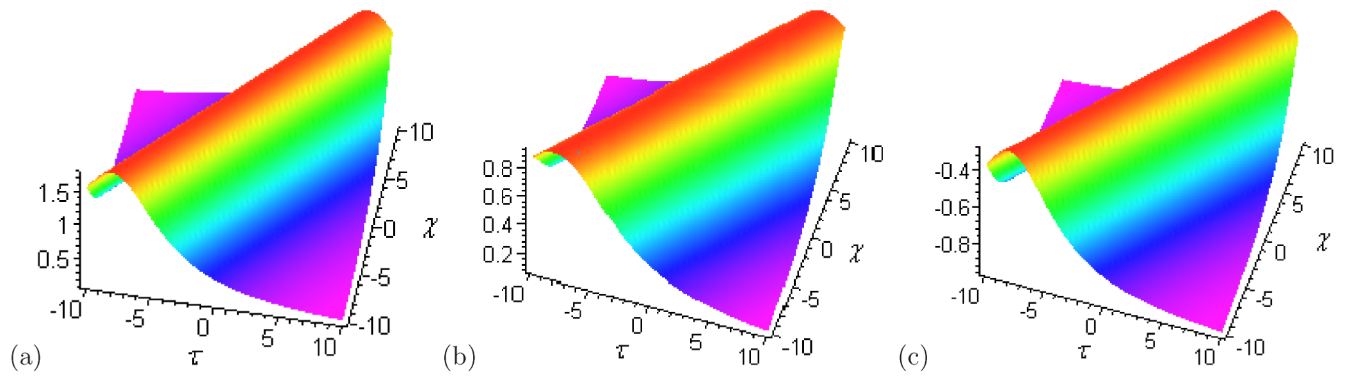

FIG. 1. (Color online) The profiles of rational solutions $|E^{[1]}{}_{r_1}|^2$, $|R^{[1]}{}_{r_1}|^2$, and $R^{z[1]}{}_{r_1}$ in Eq. (29) with specific value of $\alpha_1 = \frac{1}{3}$.

Theorem 3. Set $n = 2k$ and define $\psi_{1i}^{j,l}$ in the form

$$\psi_{1i}^{j,l} = \frac{1}{l!}\frac{\partial^l}{\partial\epsilon^l}[(\xi_1+\epsilon)^j\psi(\xi_1+\epsilon)],$$
$$i = 1,2; l = 0,1,2,\ldots,k-1;$$
$$j = 0,1,2,\ldots,n.$$

So the new expressions for a_0 and b_1 are obtained in the form

$$a_0 = \frac{\widetilde{H_{n1}}^*(-1)^{\frac{n}{2}}}{\widetilde{H_{n1}}}, \quad b_1 = -\frac{\widetilde{H_{n2}}}{\widetilde{H_{n1}}}, \tag{27}$$

where

$$\widetilde{H_{n1}} = \begin{vmatrix} \psi_{11}^{n-1,0} & \psi_{12}^{n-2,0} & \cdots & \psi_{11}^{1,0} & \psi_{12}^{0,0} \\ \psi_{12}^{*\,n-1,0} & \psi_{11}^{*\,n-2,0} & \cdots & \psi_{12}^{*\,1,0} & \psi_{11}^{*\,0,0} \\ \vdots & \vdots & \vdots & \vdots & \vdots \\ \psi_{11}^{n-1,k-1} & \psi_{12}^{n-2,k-1} & \cdots & \psi_{11}^{1,k-1} & \psi_{12}^{0,k-1} \\ \psi_{12}^{*\,n-1,k-1} & \psi_{11}^{*\,n-2,k-1} & \cdots & \psi_{12}^{*\,1,k-1} & \psi_{11}^{*\,0,k-1} \end{vmatrix},$$

$$\widetilde{H_{n2}} = \begin{vmatrix} \psi_{11}^{n,0} & \psi_{11}^{n-2,0} & \cdots & \psi_{12}^{1,0} & \psi_{11}^{0,0} \\ \psi_{12}^{*\,n,0} & \psi_{12}^{*\,n-2,0} & \cdots & \psi_{11}^{*\,1,0} & \psi_{12}^{*\,0,0} \\ \vdots & \vdots & \vdots & \vdots & \vdots \\ \psi_{11}^{n,k-1} & \psi_{11}^{n-2,k-1} & \cdots & \psi_{12}^{1,k-1} & \psi_{11}^{0,k-1} \\ \psi_{12}^{*\,n,k-1} & \psi_{12}^{*\,n-2,k-1} & \cdots & \psi_{11}^{*\,1,k-1} & \psi_{12}^{*\,0,k-1} \end{vmatrix}.$$

Proof. Under the condition of all the eigenvalues $\xi_k \longrightarrow \xi_1$, $\frac{H_{n1}^*}{H_{n1}}$ and $\frac{H_{n2}}{H_{n1}}$ degenerate into an indeterminate form $\frac{0}{0}$. So we can consider the degeneration of H_{n1} and H_{n2}, respectively. We illustrate the process as follows:

(i) For the first (second) row, we can substitute the eigenvalue ξ_1 ($\xi_2 = \xi_1^*$) and eigenfunction ψ_1 directly.

(ii) Set $\xi_3 = \xi_1 + \epsilon$ ($\xi_4 = \xi_1{}^* + \epsilon$), and do Taylor expansion in all elements of the third (fourth) with respect to ϵ, then subtracting the first (second) row from the third (fourth) row.

(iii) Considering $\xi_{2m-1} = \xi_1 + \epsilon$ (or $\xi_{2m} = \xi_1{}^* + \epsilon)(m = 3,4,\ldots,k)$ and taking the similar procedure in the $(2m-1)$th (or $2m$th) row. Note that we should do order-$(m-1)$ Taylor expansion with respect to ϵ at the $(2m-1)$th (or $2m$th) row.

(iv) Taking $\epsilon \to 0$ in a_0 and b_1, then terms with higher-order $\mathcal{O}[\epsilon^{k(k-1)+1}]$ vanish. The final expression actually implies Eq. (27).

A. The first kind of rational solutions from the vacuum

Let us consider from the vacuum $E = 0$, $R = 0$, and $R^z = -1$, the Eqs. (5) and (6) are solved by using the following eigenfunctions

$$\psi_k = \begin{pmatrix}\psi_{k1}\\ \psi_{k2}\end{pmatrix}, \quad \psi_{k1} = \exp\left[i\frac{\xi_k{}^2}{2}\left(\frac{1}{1+\xi_k^2}\chi - \tau\right)\right],$$
$$\psi_{k2} = \exp\left[-i\frac{\xi_k{}^2}{2}\left(\frac{1}{1+\xi_k^2}\chi - \tau\right)\right]. \tag{28}$$

Case (i). Substituting $\xi_1 = \alpha_1 + i\beta_1$ into Eq. (27) and letting $\beta_1 \to 0$, Eq. (25) admits the following three first-order rational solutions as follows:

$$E^{[1]}{}_{r_1} = -\frac{4\left[A_1 - i\left(\alpha_1^2+1\right)^2\right]\left(\alpha_1^2+1\right)^2\alpha_1}{\left[A_1 + i\left(\alpha_1^2+1\right)^2\right]^2} \times \exp\left[\frac{i\left(-\tau\,\alpha_1^2 - \tau + \chi\right)\alpha_1^2}{\alpha_1^2+1}\right],$$
$$R^{[1]}{}_{r_1} = -\frac{4\left[A_1 + i\left(\alpha_1^2+1\right)\left(\alpha_1^2-1\right)\right]\left(\alpha_1^2+1\right)\alpha_1}{\left[A_1 + i\left(\alpha_1^2+1\right)^2\right]^2} \times \exp\left[\frac{i\left(-\tau\,\alpha_1^2 - \tau + \chi\right)\alpha_1^2}{\alpha_1^2+1}\right], \tag{29}$$
$$R^{z[1]}{}_{r_1} = -\frac{A_1^2 + \left(\alpha_1{}^2 + 2\alpha_1 - 1\right)\left(\alpha_1{}^2 - 2\alpha_1 - 1\right)\left(\alpha_1{}^2+1\right)^2}{A_1^2 + \left(\alpha_1{}^2+1\right)^4}$$
$$A_1 = 2\alpha_1{}^2\left(\alpha_1^2+1\right)^2\tau - 2\,\alpha_1^2\,\chi.$$

Letting $\tau \to \infty$, $\chi \to \infty$, from the above, we obtain $|E^{[1]}{}_{r_1}|^2 \to 0$, $|R^{[1]}{}_{r_1}|^2 \to 0$ and $R^{z[1]}{}_{r_1} \to -1$. The trajectory of $|E^{[1]}{}_{r_1}|^2$ is defined explicitly by $\chi = (\alpha_1{}^2+1)^2\tau$ and the maximum amplitude is $16\alpha_1{}^2$. Note that $|R^{[1]}{}_{r_1}|^2$ has two peaks when $(\alpha_1{}^2 + 2\alpha_1 - 1)(\alpha_1{}^2 - 2\alpha_1 - 1) < 0$. The amplitude of $|R^{[1]}{}_{r_1}|^2$ is separately equal to $\frac{16\alpha_1{}^2(\alpha_1{}^2-1)^2}{(\alpha_1{}^2+1)^4}$ and 1 at the lines $\chi = (\alpha_1{}^2+1)^2\tau$ and $\chi = (\alpha_1{}^2+1)^2\tau \pm \frac{(\alpha_1{}^2+1)\sqrt{-(\alpha_1{}^2+2\alpha_1-1)(\alpha_1{}^2-2\alpha_1-1)}}{2\alpha_1{}^2}$. However, the amplitude of $R^{z[1]}{}_{r_1}$ occurs at the line $\chi = (\alpha_1{}^2+1)^2\tau$ and is equal to $\frac{-(\alpha_1{}^2+2\alpha_1-1)(\alpha_1{}^2-2\alpha_1-1)}{(\alpha_1{}^2+1)^2}$. In order to show the asymptotic

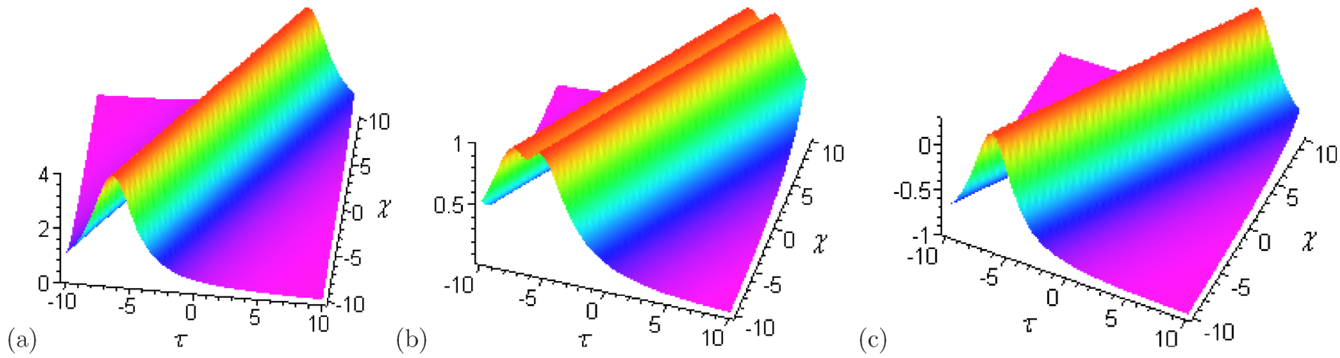

FIG. 2. (Color online) The profiles of rational solutions $|E^{[1]}{}_{r_1}|^2$, $|R^{[1]}{}_{r_1}|^2$, and $R^{z[1]}{}_{r_1}$ in Eq. (29) with $\alpha_1 = \frac{1}{2}$. Note that there are two peaks in Fig. 2(b).

properties, Figs. 1 and 2 are, respectively, plotted for the rational solutions $|E^{[1]}{}_{r_1}|^2$, $|R^{[1]}{}_{r_1}|^2$, and $R^{z[1]}{}_{r_1}$ with specific value of parameters $\alpha_1 = \frac{1}{3}$ and $\alpha_1 = \frac{1}{2}$. Note that there are two peaks in Fig. 2(b). It is trivial to know from Eq. (29) that these rational solutions $|E^{[1]}{}_{r_1}|^2$, $|R^{[1]}{}_{r_1}|^2$, and $R^{z[1]}{}_{r_1}$ exhibit algebraic decay behavior instead of exponential decay as in the case of solitons.

Case (ii). Assuming $k = 2$ and $\alpha_1 = \frac{1}{2}$ in Eqs. (25) and (27), we also construct the following three second-order rational solutions

$$\begin{aligned}
E^{[2]}{}_{r_1} &= 200\,i(-18750000 - 3840000\,\chi^2 - 9375000\,\tau^2 + 390625\,\tau^4 + 10080000\,\chi\,\tau \\
&\quad + 960000\,\chi^2\,\tau^2 - 409600\,\chi^3\,\tau - 1000000\,\tau^3\,\chi + 65536\,\chi^4 - 3125000\,i\,\tau^3 \\
&\quad + 8640000\,i\,\chi + 6000000\,i\,\chi\,\tau^2 + 819200\,i\,\chi^3 - 37500000\,i\,\tau - 3840000\,i\,\chi^2\,\tau) \\
&\quad \times (375000 - 7680\,\chi^2 - 93750\,\tau^2 + 72000\,\chi\,\tau + 4096\,i\,\chi^3 - 19200\,i\,\chi^2\,\tau \\
&\quad + 30000\,i\,\chi\,\tau^2 - 15625\,i\,\tau^3 - 187500\,i\,\tau + 177600\,i\,\chi)\exp(1/20\,i\,(-5\,\tau + 4\,\chi))/(P_1 + i\,P_2)^2 \\
R^{[2]}{}_{r_1} &= -160\,\exp(1/20\,i\,(-5\,\tau + 4\,\chi))(-751875000000\,\chi\,\tau^4 + 780000000000\,\chi^2\,\tau^3 - 394752000000\,\chi^3\,\tau^2 \\
&\quad + 96829440000\,\chi^4\,\tau - 35840000000\,\chi^4\,\tau^3 - 52500000000\,\chi^2\,\tau^5 + 56000000000\,\chi^3\,\tau^4 + 13762560000\,\chi^5\,\tau^2 \\
&\quad - 2936012800\,\chi^6\,\tau + 27343750000\,\chi\,\tau^6 + 268435456\,\chi^7 - 6997500000000\,\chi\,\tau^2 + 2520000000000\,\chi^2\,\tau \\
&\quad + 266015625000\,i\,\tau^4 + 80566406250\,i\,\tau^6 + 3192187500000\,i\,\tau^2 + 2160000000000\,i\,\chi^2 - 290625000000\,i\,\tau^5\,\chi \\
&\quad - 36175872000\,i\,\chi^5\,\tau - 345600000000\,i\,\chi^3\,\tau^3 - 1035000000000\,i\,\tau^3\,\chi - 448512000000\,i\,\chi^3\,\tau \\
&\quad - 7290000000000\,i\,\tau\,\chi - 365568000000\,\chi^3 + 5725781250000\,\tau^3 + 284179687500\,\tau^5 - 9122611200\,\chi^5 \\
&\quad - 6103515625\,\tau^7 + 3870000000000\,\chi - 10659375000000\,\tau + 71368704000\,i\,\chi^4 + 3523215360\,i\,\chi^6 \\
&\quad + 1080000000000\,i\,\chi^2\,\tau^2 + 435000000000\,i\,\tau^4\,\chi^2 + 153600000000\,i\,\chi^4\,\tau^2 - 1181250000000\,i)/(P_1 + i\,P_2)^2, \\
R^{z[2]}{}_{r_1} &= -(-102400000000\,\chi^3\,\tau^3 - 360000000000\,\tau^4\,\chi^2 + 188743680000\,\chi^5\,\tau + 1125000000000\,\tau^5\,\chi \\
&\quad - 147456000000\,\chi^4\,\tau^2 - 917504000000\,\chi^5\,\tau^3 + 1792000000000\,\tau^4\,\chi^4 - 2240000000000\,\tau^5\,\chi^3 \\
&\quad - 781250000000\,\tau^7\,\chi + 1750000000000\,\tau^6\,\chi^2 + 293601280000\,\chi^6\,\tau^2 - 53687091200\,\chi^7\,\tau \\
&\quad - 296437500000000 - 683593750000\,\tau^6 - 160200000000000\,\chi\,\tau + 156960000000000\,\chi^2\,\tau^2 \\
&\quad - 56156160000000\,\chi^3\,\tau - 175500000000000\,\tau^3\,\chi + 4294967296\,\chi^8 + 152587890625\,\tau^8 \\
&\quad + 167040000000000\,\chi^2 + 249581250000000\,\tau^2 + 72117187500000\,\tau^4 + 7066091520000\,\chi^4 \\
&\quad - 46976204800\,\chi^6)/\left(P_1{}^2 + P_2{}^2\right),
\end{aligned}$$

$$\begin{aligned}
\text{with}\quad P_1 &= 18750000 + 3840000\,\chi^2 + 9375000\,\tau^2 - 390625\,\tau^4 - 10080000\,\chi\,\tau \\
&\quad - 960000\,\chi^2\,\tau^2 + 409600\,\chi^3\,\tau + 1000000\,\tau^3\,\chi - 65536\,\chi^4, \\
P_2 &= -3125000\,\tau^3 + 8640000\,\chi + 6000000\,\chi\,\tau^2 + 819200\,\chi^3 - 37500000\,\tau - 3840000\,\chi^2\,\tau. \qquad (30)
\end{aligned}$$

The dynamical evolution of $|E^{[2]}{}_{r_1}|^2$, $|R^{[2]}{}_{r_1}|^2$, and $R^{z[2]}{}_{r_1}$ are given in the Fig. 3. According to the physical meaning of the rotating RMB equations, these rational solutions can also be called as rational few cycle optical solitons, which have never been reported in the literature.

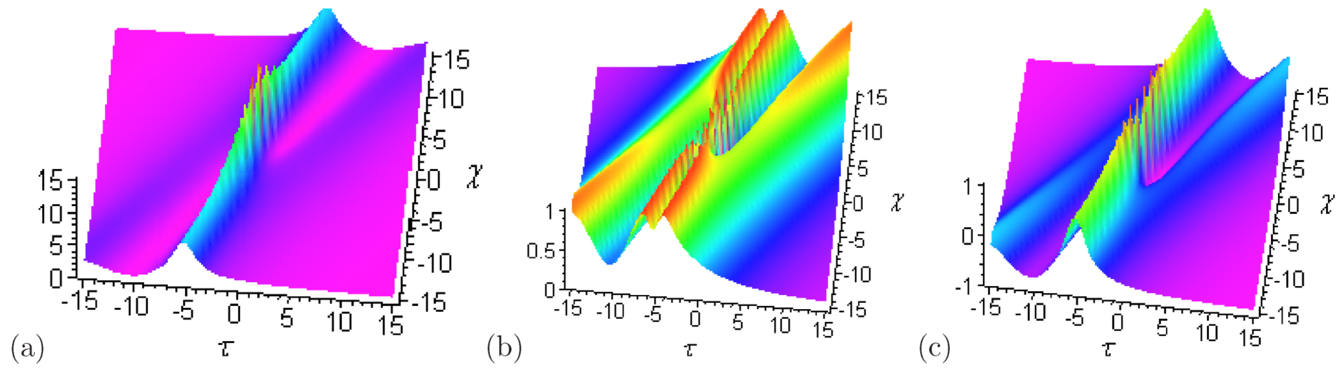

FIG. 3. (Color online) The dynamical evolution of the second-order rational solutions $|E^{[2]}{}_{r_1}|^2$, $|R^{[2]}{}_{r_1}|^2$, and $R^{z[2]}{}_{r_1}$ in Eq. (30).

B. The second kind of rational solutions from the monochromatic wave

Let a, b, and c be three real constants, then substituting $E = c\exp\left[i(a\tau + b\chi)\right]$, $R = -\frac{bc}{a}\exp\left[i(a\tau + b\chi)\right]$, and $R^z = -\frac{b(a-1)}{a}$ into the spectral problem Eqs. (5) and (6), and using the method of separation of variables and the superposition principle, the eigenfunction ψ_k associated with ξ_k is given by

$$\begin{pmatrix}\psi_{k1}(\tau,\chi,\xi_k)\\ \psi_{k2}(\tau,\chi,\xi_k)\end{pmatrix} = \begin{pmatrix}C_1\varpi_1(\tau,\chi,\xi_k)[1] + C_2\varpi_2(\tau,\chi,\xi_k)[1] + C_3\varpi_1^*(\tau,\chi,\xi_k^*)[2] + C_4\varpi_2^*(\tau,\chi,\xi_k^*)[2]\\ C_1\varpi_1(\tau,\chi,\xi_k)[2] + C_2\varpi_2(\tau,\chi,\xi_k)[2] + C_3\varpi_1^*(\tau,\chi,\xi_k^*)[1] + C_4\varpi_2^*(\tau,\chi,\xi_k^*)[1]\end{pmatrix}. \tag{31}$$

Here

$$\begin{pmatrix}\varpi_1(\tau,\chi,\xi_k)[1]\\ \varpi_1(\tau,\chi,\xi_k)[2]\end{pmatrix} = \begin{pmatrix}\exp\left(-iK(\xi_k)\frac{a\tau+a\xi_k{}^2\tau+b\chi}{2(1+\xi_k{}^2)a} + \frac{1}{2}i\theta\right)\\ -i\frac{-a-\xi_k{}^2+K(\xi_k)}{\xi_k c}\exp\left(-iK(\xi_k)\frac{a\tau+a\xi_k{}^2\tau+b\chi}{2(1+\xi_k{}^2)a} - \frac{1}{2}i\theta\right)\end{pmatrix},$$

$$\begin{pmatrix}\varpi_2(\tau,\chi,\xi_k)[1]\\ \varpi_2(\tau,\chi,\xi_k)[2]\end{pmatrix} = \begin{pmatrix}\exp\left(iK(\xi_k)\frac{a\tau+a\xi_k{}^2\tau+b\chi}{2(1+\xi_k{}^2)a} + \frac{1}{2}i\theta\right)\\ i\frac{a+\xi_k{}^2+K(\xi_k)}{\xi_k c}\exp\left(iK(\xi_k)\frac{a\tau+a\xi_k{}^2\tau+b\chi}{2(1+\xi_k{}^2)a} - \frac{1}{2}i\theta\right)\end{pmatrix},$$

$$\varpi_1(\tau,\chi,\xi_k) = \begin{pmatrix}\varpi_1(\tau,\chi,\xi_k)[1]\\ \varpi_1(\tau,\chi,\xi_k)[2]\end{pmatrix},\quad \varpi_2(\tau,\chi,\xi_k) = \begin{pmatrix}\varpi_2(\tau,\chi,\xi_k)[1]\\ \varpi_2(\tau,\chi,\xi_k)[2]\end{pmatrix},$$

$$K(\xi_k) = \sqrt{a^2 + 2a\xi_k{}^2 + \xi_k{}^4 - \xi_k{}^2c^2},\quad \theta = a\tau + b\chi,$$

and $a, b, c, \tau, \chi \in \mathbb{R}$, $C_1, C_2, C_3, C_4 \in \mathbb{C}$. Note that $\varpi_1(\tau,\chi,\xi_k)$ and $\varpi_2(\tau,\chi,\xi_k)$ are two linear independent solutions.

In order to derive the second kind of rational solutions, i.e., the rogue wave solutions, of the RMB equations, a crucial step is to find a common zero point of K and the eigenfunctions ψ_k such that exponential functions vanish and the indeterminate form $\frac{0}{0}$ appear in Eq. (27) as in the case of the NLS equation [57]. After tedious calculations, we observe the following fact: By setting

$$\begin{aligned}
C_1 &= -1 + i(K_0+1) + \exp\left[\frac{1}{2}iK(\xi_k)\sum_{j=0}^{k-1}S_j(\xi_k-\xi_0)^j\right],\\
C_2 &= -1 + i(K_0+1) + \exp\left[-\frac{1}{2}iK(\xi_k)\sum_{j=0}^{k-1}S_j(\xi_k-\xi_0)^j\right],\\
C_3 &= K_0 + \exp\left[\frac{1}{2}iK(\xi_k)\sum_{j=0}^{k-1}L_j(\xi_k-\xi_0)^j\right],\\
C_4 &= K_0 + \exp\left[-\frac{1}{2}iK(\xi_k)\sum_{j=0}^{k-1}L_j(\xi_k-\xi_0)^j\right],
\end{aligned} \tag{32}$$

then $\xi_0 = \frac{c}{2} + i\frac{\sqrt{4a-c^2}}{2}$ is only one zero point of K and eigenfunction ψ_k in Eq. (31). Here $K_0, S_j, L_j \in \mathbb{C}$. Because ξ_0 is a zero point of eigenfunction ψ_k, we must add first-order derivatives of every row in determinants of Eq. (27). Letting $\xi_1 \to \xi_0$, the second kind of rational solutions, i.e., the rogue waves, can be constructed from Eqs. (25), (27), (31), and (32).

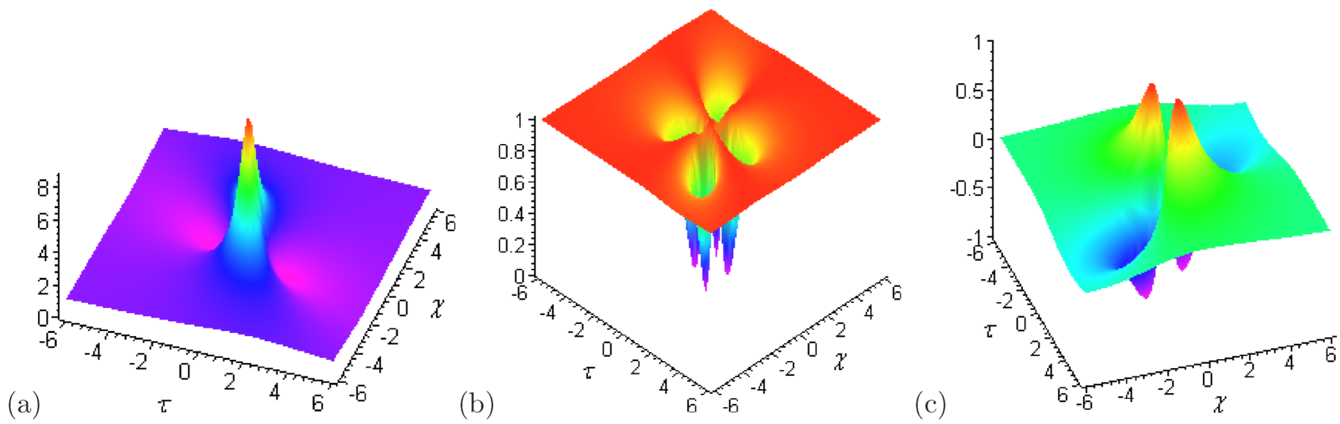

FIG. 4. (Color online) The dynamical evolution of the first-order rogue waves $|E^{[1]}{}_{r_2}|^2$, $|R^{[1]}{}_{r_2}|^2$, and $R^{z[1]}{}_{r_2}$ in Eq. (33). These pictures clearly show the asymptotic localized property and large amplitude of the rogue wave.

Case (iii). For simplicity, let $a = b = c = 1$, $K_0 = S_0 = L_0 = 0$, Eqs. (25) and (27) reduce to rogue wave solutions of the following form:

$$\begin{aligned} E^{[1]}{}_{r_2} &= -\frac{\exp[i(\chi+\tau)](\chi^2+\chi\tau+\tau^2+1+i\tau)(\chi^2+\chi\tau+\tau^2-3+i\tau+4i\chi)}{(-\chi^2-\chi\tau-\tau^2-1+i\tau)^2},\\ R^{[1]}{}_{r_2} &= \frac{\exp[i(\chi+\tau)](\chi^2+\chi\tau+2i\chi+\tau^2+3i\tau-1)(\chi^2+\chi\tau+2i\chi+\tau^2-i\tau-1)}{(-\chi^2-\chi\tau-\tau^2-1+i\tau)^2},\\ R^{z[1]}{}_{r_2} &= \frac{4\tau(2\chi+\tau)}{(\chi^2+\chi\tau+\tau^2+1)^2+\tau^2}. \end{aligned} \tag{33}$$

Figure 4 is plotted for $|E^{[1]}{}_{r_2}|^2$, $|R^{[1]}{}_{r_2}|^2$, and $R^{z[1]}{}_{r_2}$. From Fig. 4(a), we infer that $|E^{[1]}{}_{r_2}|^2 \to 1$ by setting $\tau \to \infty$, $\chi \to \infty$, which gives an asymptotic plane, and the maximum amplitude of $|E^{[1]}{}_{r_2}|^2$ is equal to 9, which occurs at the coordinate origin ($\tau = 0$, $\chi = 0$), and the minimum amplitude of $|E^{[1]}{}_{r_2}|^2$ is equal to 0, which occurs at two points ($\tau = -\frac{4\sqrt{39}}{13}, \chi = \frac{\sqrt{39}}{13}$) and ($\tau = \frac{4\sqrt{39}}{13}, \chi = -\frac{\sqrt{39}}{13}$). In Fig. 4(b), we observe that the height of the asymptotical plane is 1 because $|R^{[1]}{}_{r_2}|^2 \to 1$ when $\tau \to \infty$, $\chi \to \infty$, and the maximum amplitude of $|R^{[1]}{}_{r_2}|^2$ occurs at the two lines $\tau = 0$ and $\chi = -\frac{\tau}{2}$, and is equal to 1. These two lines match quickly with the asymptotical plane at the same height, such that the localized property of $|R^{[1]}{}_{r_2}|^2$ is preserved. The minimum amplitude of $|R^{[1]}{}_{r_2}|^2$ is equal to 0, which occurs at four points ($\tau = -\frac{2\sqrt{7}}{7}, \chi = \frac{3\sqrt{7}}{7}$), ($\tau = \frac{2\sqrt{7}}{7}, \chi = -\frac{3\sqrt{7}}{7}$), ($\tau = \frac{2\sqrt{7}}{7}, \chi = \frac{\sqrt{7}}{7}$), and ($\tau = -\frac{2\sqrt{7}}{7}, \chi = -\frac{\sqrt{7}}{7}$). From Fig. 4(c), we conclude that the height of the asymptotical plane is 0, the maximum amplitude of $R^{z[1]}{}_{r_2}$ is located at ($\tau = \frac{2\sqrt{7}}{7}, \chi = \frac{\sqrt{7}}{7}$), ($\tau = -\frac{2\sqrt{7}}{7}, \chi = -\frac{\sqrt{7}}{7}$) and is equal to 1, and the minimum amplitude of $R^{z[1]}{}_{r_2}$ is located at ($\tau = -\frac{2\sqrt{7}}{7}, \chi = \frac{3\sqrt{7}}{7}$), ($\tau = \frac{2\sqrt{7}}{7}, \chi = -\frac{3\sqrt{7}}{7}$) and is equal to -1. Finally, the extreme value of the amplitude $R^{z[1]}{}_{r_2}$ occurs at point ($\tau = 0$, $\chi = 0$) and is equal to 0. To show the localized distribution on (x,t) plane of the first-order rogue waves, we give their density plots in Fig. 5. Furthermore, taking eigenfunctions in Eq. (31) back into Eq. (25), the first-order breather solutions of the rotating RMB equations are obtained, which are plotted in Fig. 6 for the same parameters

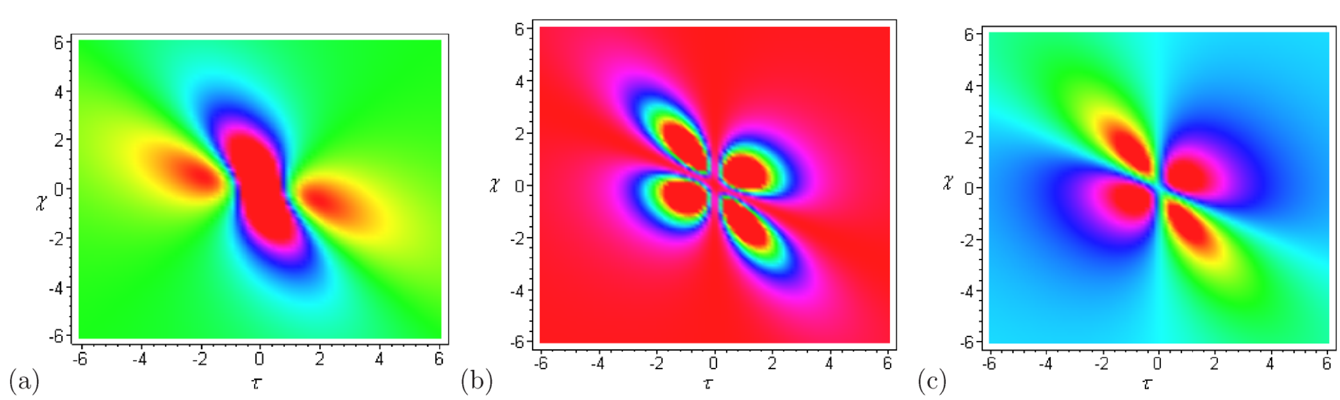

FIG. 5. (Color online) The corresponding density plots of pictures described in the legend of Fig. 4.

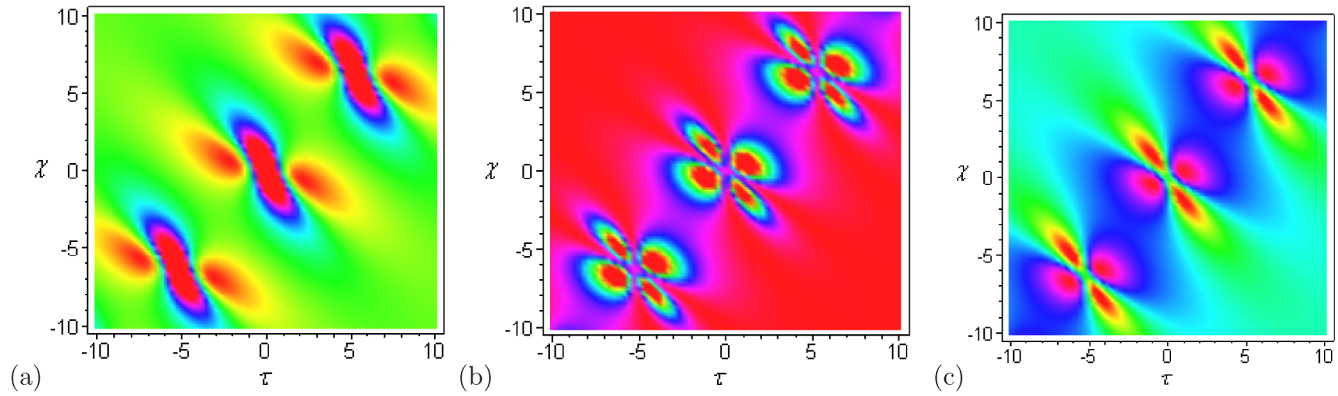

FIG. 6. (Color online) Density plots of the first-order breathers $|E^{[1]}|^2$, $|R^{[1]}|^2$, and $R^{z[1]}$. These solutions are plotted by taking Eq. (31) into Eq. (25) for the same parameters as described in the legend of Fig. 4, except $\beta_1 = \frac{3}{4}$. Note that the central peaks look very similar to the corresponding profiles of rogue waves as described in the legend of Fig. 5.

in Fig. 4 except $\beta_1 = \frac{3}{4}$. Under this choice, the eigenfunction ψ_1 does not have zero point thus allows smooth breathers by DT. This can be verified visually by comparing Figs. 5 and 6.

Case (iv). To further illustrate the construction method of the different-order rogue waves, we shall provide the second-order and third-order rogue waves of the rotating RMB equations. Setting $k = 2$, $a = b = c = 1$, $K_0 = S_0 = S_1 = L_0 = 0$, $L_1 = 50$ in Eqs. (25), (27), (31), and (32), we get the second-order rogue waves in triangular pattern as follows:

$$\begin{aligned}
E^{[2]}{}_{r_2} =\ & \exp((\tau+\chi)i)(6\chi^4\tau^2 + 3\chi^5\tau + 3\chi\tau^5 + 7\chi^3\tau^3 + 6\tau^4\chi^2 - 78\chi^3\tau - 33\chi\tau^3 - 9\chi\tau + 450\chi^2\tau \\
& - 54\tau^2\chi^2 - 45i\tau - 36i\chi - 15i\tau^3 - 120i\chi^3 + 12i\chi^5 + 750i\chi^2 + 300i\tau^2 + 3i\tau^5 - 90i\tau\chi^2 - 57\chi^4 \\
& + 150\chi^3 - 12\tau^4 + \chi^6 + \tau^6 - 150\tau^3 + 99\chi^2 - 72\tau^2 + 7545 - 450i - 1650\tau - 1650\chi + 54i\tau^2\chi + 18i\chi\tau^4 \\
& + 33i\chi^2\tau^3 + 42i\tau^2\chi^3 + 27i\chi^4\tau + 2100i\tau\chi)(6\chi^4\tau^2 + 3\chi^5\tau + 3\chi\tau^5 + 7\chi^3\tau^3 + 6\tau^4\chi^2 + 18\chi^3\tau \\
& + 15\chi\tau^3 - 9\chi\tau + 450\chi^2\tau + 54\tau^2\chi^2 - 300i\tau^2 + 3i\tau^5 + 150i\chi^2 + 27i\tau + 9i\tau^3 - 300i\tau\chi + 3\chi^4 \\
& + 150\chi^3 + \chi^6 + \tau^6 - 150\tau^3 + 27\chi^2 + 36\tau^2 + 750\tau - 450\chi + 18i\tau^2\chi + 6i\chi\tau^4 \\
& + 6i\tau^2\chi^3 + 3i\chi^4\tau + 9i\tau^3\chi^2 + 54i\chi^2\tau + 7509 + 150i)/(Q_1 + iQ_2)^2, \\
R^{[2]}{}_{r_2} =\ & -\exp((\tau+\chi)i)(-12i\chi^3 - 18i\chi - 3i\tau^5 + 7491 + 750i + 6\chi^4\tau^2 + 3\chi^5\tau + 3\chi\tau^5 + 7\chi^3\tau^3 + 6\chi^3\tau \\
& + 15\chi\tau^3 + 27\chi\tau + 450\chi^2\tau + 36\tau^2\chi^2 + 150i\chi^2 + 600i\tau^2 + 6i\chi^5 + 3i\tau^3 + 6\tau^4\chi^2 - 18i\tau\chi^2 - 15\chi^4 \\
& + 150\chi^3 - 6\tau^4 + \chi^6 + \tau^6 - 150\tau^3 - 9\chi^2 - 54\tau^2 + 150\tau + 150\chi + 45i\tau + 72i\tau^2\chi + 12i\tau^2\chi^3 + 9i\chi^4\tau \\
& + 1500i\tau\chi + 3i\chi^2\tau^3)(-12i\chi^3 - 18i\chi - 33i\tau^3 - 600i\tau^2 + 6\chi^4\tau^2 + 3\chi^5\tau + 3\chi\tau^5 + 7\chi^3\tau^3 + 6\tau^4\chi^2 \\
& - 42\chi^3\tau - 57\chi\tau^3 - 117\chi\tau + 450\chi^2\tau - 36\tau^2\chi^2 + 750i\chi^2 + 6i\chi^5 + 9i\tau + 9i\tau^5 + 7491 + 150i \\
& - 15\chi^4 + 150\chi^3 - 30\tau^4 + \chi^6 + \tau^6 - 150\tau^3 - 9\chi^2 + 18\tau^2 + 1350\tau - 1050\chi + 54i\chi^2\tau \\
& + 300i\tau\chi + 24i\chi\tau^4 + 39i\chi^2\tau^3 + 36i\tau^2\chi^3 + 21i\chi^4\tau)/(Q_1 + iQ_2)^2, \\
R^{z[2]}{}_{r_2} =\ & 12(-22500 + 486\chi^4\tau^2 + 108\chi^5\tau + 270\chi\tau^5 + 360\chi^3\tau^3 + 270\tau^4\chi^2 - 59928\chi^3\tau - 120216\chi\tau^3 \\
& - 299838\chi\tau + 12600\chi^2\tau - 134244\tau^2\chi^2 - 22500\tau^2\chi - 6600\chi\tau^4 - 9600\chi^2\tau^3 - 3000\tau^2\chi^3 + 4800\chi^4\tau \\
& + 7500\chi^4 + 600\chi^5 + 600\chi^3 - 30126\tau^4 - 9\tau^6 - 600\tau^3 + 45000\chi^2 + 74865\tau^2 - 2400\tau^5 + 746400\tau \\
& - 748200\chi + 54\chi^5\tau^5 + 9\chi^8\tau^2 + 24\chi^7\tau^3 + 2\chi^9\tau + 18\chi^2\tau^8 + 6\chi\tau^9 + 51\chi^4\tau^6 \\
& + 36\chi^3\tau^7 + 42\chi^6\tau^4 - 600\chi^2\tau^5 + 108\chi\tau^7 + 162\chi^2\tau^6 + 198\chi^4\tau^4 + 216\chi^5\tau^3 \\
& + 72\chi^7\tau + 500\chi\tau^6 - 3400\chi^4\tau^3 + 180\chi^6\tau^2 - 200\chi^6\tau - 2600\chi^3\tau^4 - 2100\chi^5\tau^2 \\
& + 180\chi^3\tau^5 + 200\chi^7 + \tau^{10} + 100\tau^7 + 18\tau^8)/\left(Q_1{}^2 + Q_2{}^2\right), \\
\text{with}\, Q_1 =\ & -6\chi^4\tau^2 - 3\chi^5\tau - 3\chi\tau^5 - 7\chi^3\tau^3 - 6\tau^4\chi^2 - 18\chi^3\tau - 15\chi\tau^3 + 9\chi\tau - 450\chi^2\tau - 54\tau^2\chi^2 \\
& - 3\chi^4 - 150\chi^3 - \chi^6 - \tau^6 + 150\tau^3 - 27\chi^2 - 36\tau^2 - 750\tau + 450\chi - 7509, \\
Q_2 =\ & -300\tau^2 + 3\tau^5 + 150\chi^2 + 27\tau + 9\tau^3 - 300\tau\chi + 18\tau^2\chi + 6\chi\tau^4 + 6\tau^2\chi^3 + 3\chi^4\tau \\
& + 9\tau^3\chi^2 + 54\chi^2\tau + 150.
\end{aligned} \qquad (34)$$

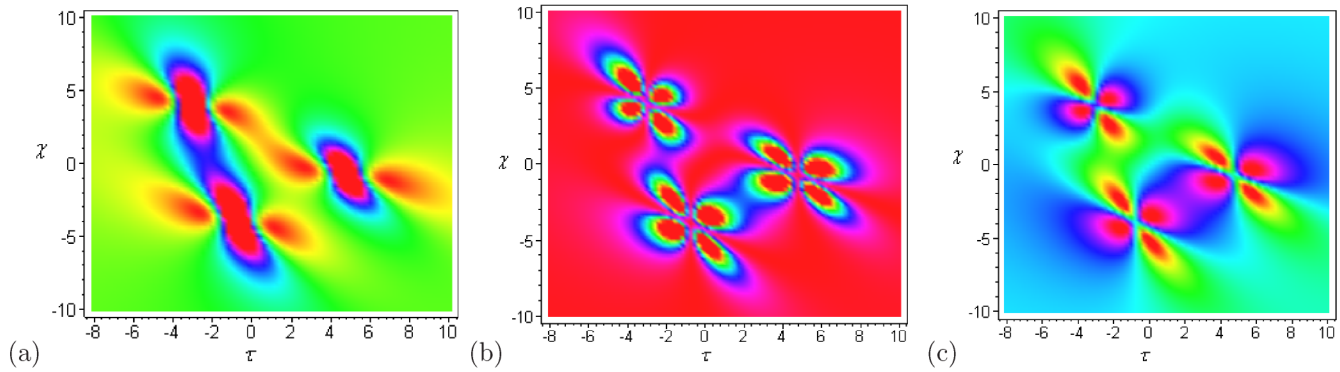

FIG. 7. (Color online) Density plots of triangular pattern of the second-order rogue waves $|E^{[2]}{}_{r_2}|^2$, $|R^{[2]}{}_{r_2}|^2$, and $R^{z[2]}{}_{r_2}$ in Eq. (34).

These solutions are plotted in Fig. 7. Similarly, choosing $a = b = c = 1$, $K_0 = S_0 = S_1 = S_2 = L_0 = 0$ for the third-order rogue waves solutions $|E^{[3]}{}_{r_2}|^2$, $|R^{[3]}{}_{r_2}|^2$, and $R^{z[3]}{}_{r_2}$, Fig. 8 is plotted for triangular pattern with $L_1 = 100$, $L_2 = 0$, but Fig. 9 is plotted for circular pattern with $L_1 = 0$, $L_2 = 800$. Figures 8 and 9 show that profiles of the rogue waves could be changed dramatically only by selecting the values of combination coefficients $C_i (i = 1, 2, 3, 4)$ through L_1 and L_2. Needless to say, we have also constructed analytical formulas of the third-order rogue waves, but it is too long to present here. It is possible to get more interesting patterns from the higher-order rogue waves of the rotating RMB equations as we have done for the NLS equation [57]. According to the physical meaning of the rotating RMB equations, solutions above are actually few-cycle optical rogue waves, which are derived for the first time. As we have discussed in the introduction, the RMB equation has been analyzed for the past four decades and different solutions have been reported, including highly localized soliton solutions. In particular, in the case of SIT-type solitons, the theoretical results about the existence of solitons have been experimentally supported by several groups. However, the rogue-type rational solutions have not been reported for RMB equations. In addition to the above, the multi-rogue wave solutions have not been reported for this equation. In all the published results on RMB equations so far, it is well documented that the non-SVEA method has been widely used to develop the system of governing equation and several interesting results have been reported. As the non-SVEA method is mainly used for ultrashort few-cycle optical pulse propagation through nonlinear optical media, we strongly believe that the results of this paper will be very useful to understand and analyze the generation of high-power laser pulses in optics as well as their evolution by suitably choosing the pulse parameters.

C. The reflections of the rogue waves on the electric fields

We know from the above results that E has rogue waves, but the real physical fields in ultrashort pulse are two polarized electric fields ϵ_x and ϵ_y. So it is essential for us to find the reflections of the rogue waves on them or equivalently on $E_x = \frac{2d}{\hbar\omega_0}\varepsilon_x$ (the real part of E) and $E_y = \frac{2d}{\hbar\omega_0}\varepsilon_y$(the imaginary part of E). Figures 10–13 are density plots for the real and imaginary parts of all rogue waves of E, respectively. In these figures, a green bar denotes a vale and a purple bar denotes a upward ridge in profiles of E_x and E_y. A group of red bright points (GRBPs) in green area denotes a downward peak, but a GRBPs in purple area denotes a peak in upward ridge. In general, a GRBPs for two cases denotes a localized large amplitude oscillation of a polarized electric field. In most cases, two kinds of GRBPs are paired except the one in Fig. 10(a). By comparing Figs. 5(a), 7(a), 8(a), and 9(a) with Figs. 10–13 in order, it is easy to find that the patterns of the GRBPs (or paired GRBPs) are similar to the

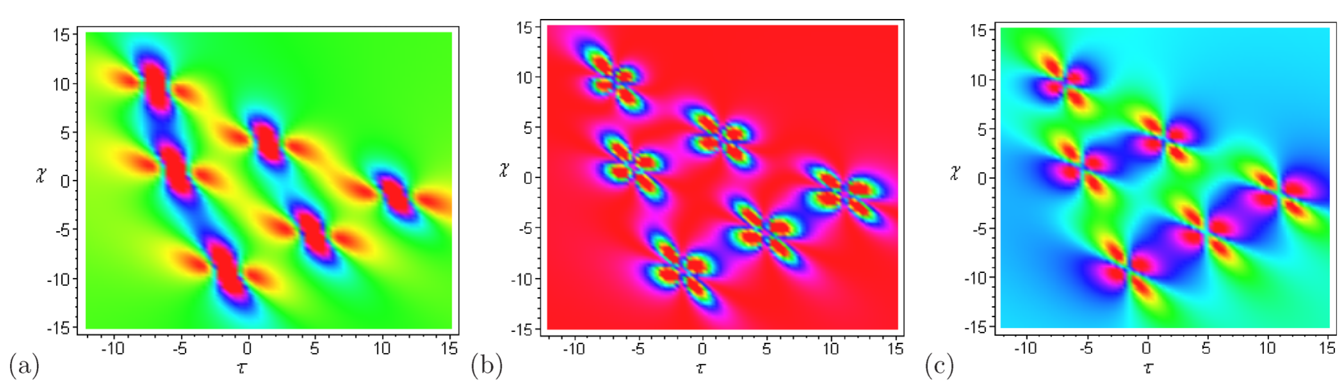

FIG. 8. (Color online) Density plots of triangular pattern of the third-order rogue waves $|E^{[3]}{}_{r_2}|^2$, $|R^{[3]}{}_{r_2}|^2$, and $R^{z[3]}{}_{r_2}$, with parameters $a = b = c = 1$, $K_0 = S_0 = S_1 = S_2 = L_0 = 0$, $L_1 = 100$, $L_2 = 0$.

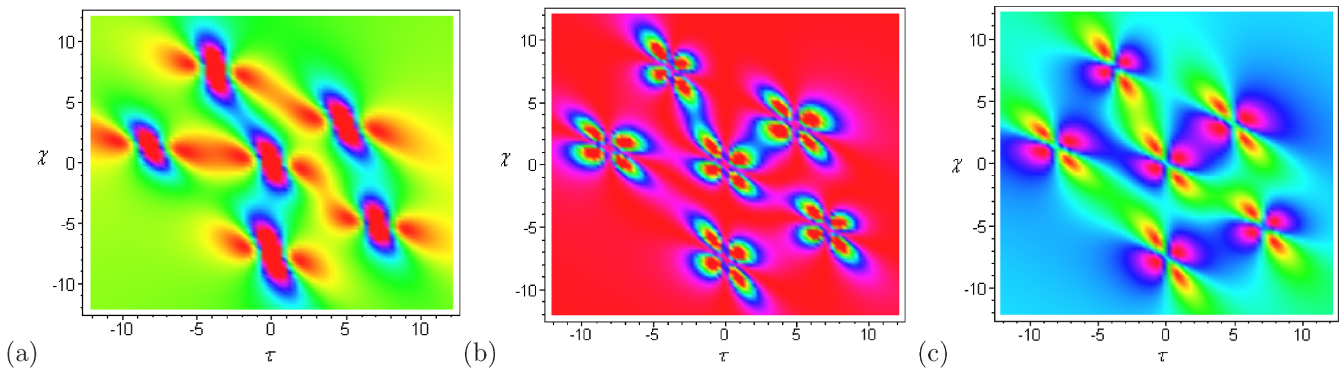

FIG. 9. (Color online) Density plots of the third-order rogue waves $|E^{[3]}{}_{r_2}|^2$, $|R^{[3]}{}_{r_2}|^2$, and $R^{z[3]}{}_{r_2}$ with same values of parameters as described in the legend of Fig. 8, except $L_1 = 0$, $L_2 = 800$.

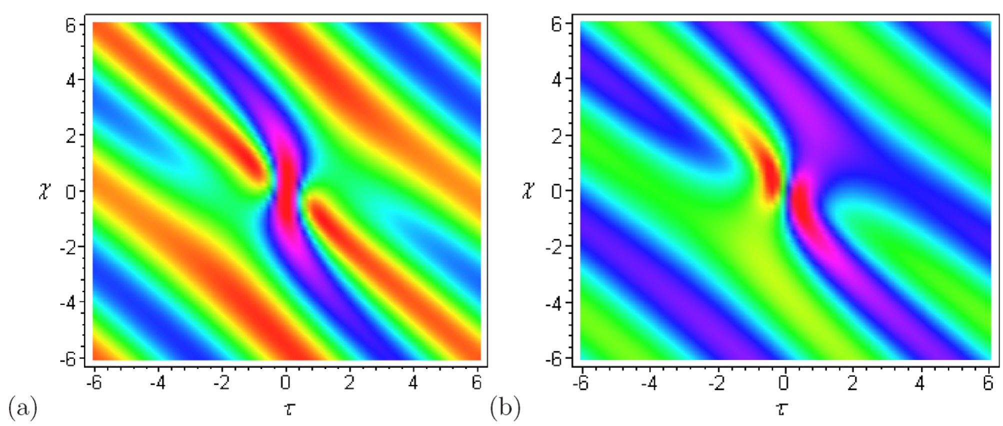

FIG. 10. (Color online) Density plots of $E^{[1]}{}_{r_2,x}$(real part of $E^{[1]}{}_{r_2}$) and $E^{[1]}{}_{r_2,y}$(imaginary part of $E^{[1]}{}_{r_2}$) for the values described in the legend of Fig. 5.

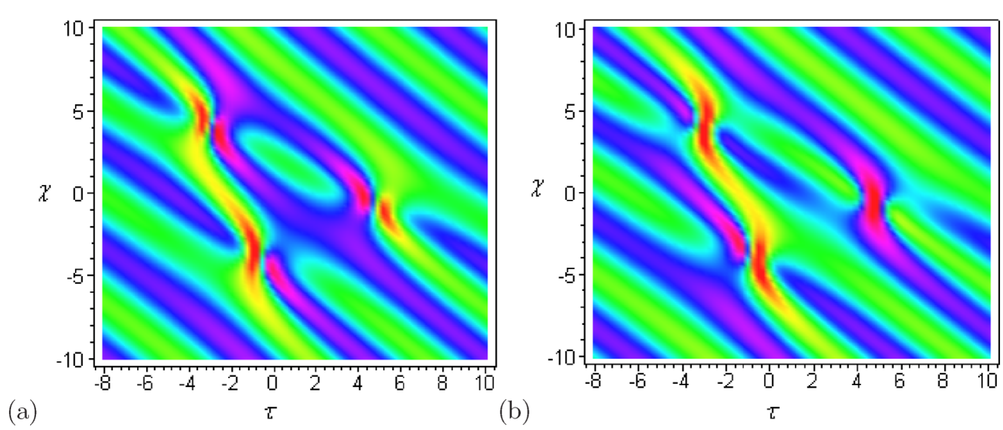

FIG. 11. (Color online) Density plots of $E^{[2]}{}_{r_2,x}$ (real part of $E^{[2]}{}_{r_2}$) and $E^{[2]}{}_{r_2,y}$ (imaginary part of $E^{[2]}{}_{r_2}$) for the values described in the legend of Fig. 7.

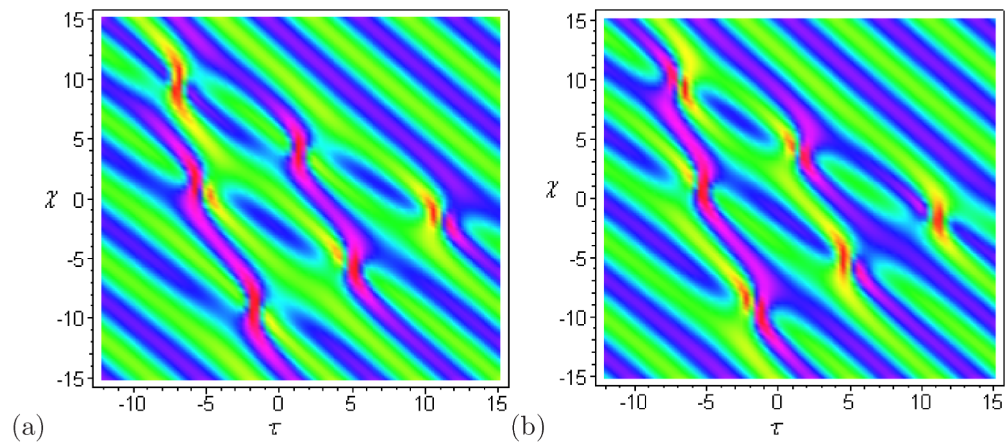

FIG. 12. (Color online) Density plots of $E^{[3]}{}_{r_2,x}$ (real part of $E^{[3]}{}_{r_2}$) and $E^{[3]}{}_{r_2,y}$ (imaginary part of $E^{[3]}{}_{r_2}$) for the values described in the legend of Fig. 8.

corresponding patterns of rogue waves of $|E|^2$; thus, we think a paired GRBPs corresponds to a first-order rogue wave. In other words, the GRBPs (or paired GRBPs), or a localized large amplitude oscillation is the first reflection of the rogue wave on the two polarized electric fields.

According to the analytical formulas of rogue waves $E^{[j]}{}_{r_2}(j = 1,2,3)$, and setting $\tau \rightarrow \infty$, $\chi \rightarrow \infty$, then $E^{[j]}{}_{r_2,x} = -\cos(\tau + \chi)$, $E^{[j]}{}_{r_2,y} = -\sin(\tau + \chi)$ for $j = 1$ and $j = 3$, but $E^{[2]}{}_{r_2,x} = \cos(\tau + \chi)$, $E^{[2]}{}_{r_2,y} = \sin(\tau + \chi)$, which is the second reflection of the localized property of rogue wave. Thus, there is a complementary relationship of two electric field components E_x and E_y when χ and τ are sufficiently large. This can be verified by the alterative appearance of blue and purple bars in Figs. 10–13.

IV. SUMMARY AND DISCUSSION

In this article, we have reported the determinant representation of DT for the rotating RMB equations associated with SIT effect and the propagation of few-cycle pulses. By using the degenerate DT, we have constructed two kinds of rational solutions, i.e., rational solitons and multi-rogue wave of rotating RMB equations. The two lowest-order rational solitons and rogue wave solutions are given explicitly and plotted in figures. The triangular and circular patterns of the third-order rogue waves are also analyzed in detail. The obtained solutions have also been confirmed by symbolic computation and validated, this forms the main results of the work. We have found two reflections of rogue wave on the polarized electric fields: (1) a localized large amplitude oscillation on a periodic background; (2) a complementary relationship of two electric field components E_x and E_y when χ and τ are sufficiently large. Note that the periodic background is given by the asymptotical behavior of E_x and E_y of rogue waves. From the physical point of view of the rotating RMB equations, these solutions are actually rational type few-cycle optical solitons and few-cycle optical rogue waves. Our solutions open several new avenues in the area of ultrashort pulse dynamics in optics. As rogue wave-type solutions have been observed in many branches of physics, the results of this paper may be useful to explore the production of high-power few-cycle optical pulses for different applications in optics, in particular, in the area of near-field nonlinear optics and fabrication of new optical white light coherent sources.

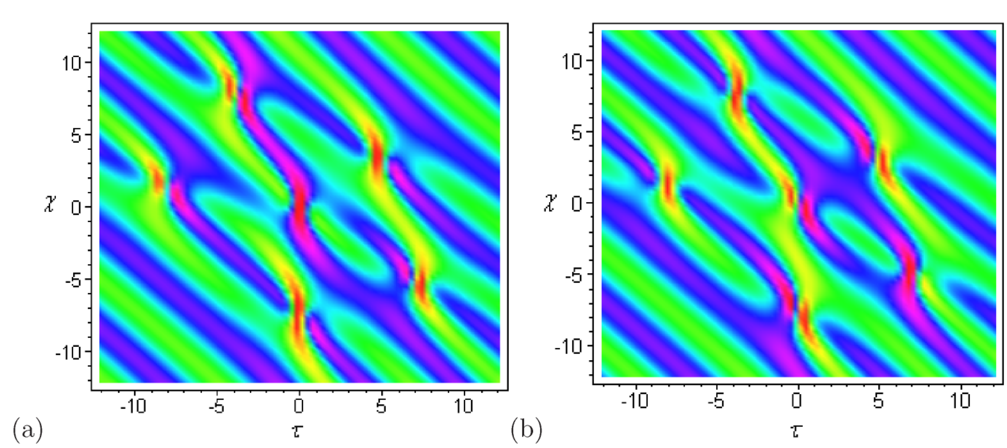

FIG. 13. (Color online) Density plots of $E^{[3]}{}_{r_2,x}$ (real part of $E^{[3]}{}_{r_2}$) and $E^{[3]}{}_{r_2,y}$ (imaginary part of $E^{[3]}{}_{r_2}$) for the values described in the legend of Fig. 9.

ACKNOWLEDGMENTS

This work is supported by the NSF of China under Grant No. 11271210 and K. C. Wong Magna Fund in Ningbo University. J.H. is also supported by the Natural Science Foundation of Ningbo under Grant No. 2011A610179. J.H. thanks Professsor A. S. Fokas for arranging the visit to Cambridge University and for many useful discussions. K.P. thanks the DST and CSIR, Government of India, for the financial support through major projects.

APPENDIX A: THE MATRIX FORM OF THE ONEFOLD DARBOUX MATRIX

Considering the universality of DT, the trial Darboux matrix T in Eq. (7) is assumed to be of the form

$$T = T(\xi) = \begin{pmatrix} a_1 & b_1 \\ c_1 & d_1 \end{pmatrix} \xi + \begin{pmatrix} a_0 & b_0 \\ c_0 & d_0 \end{pmatrix}, \tag{A1}$$

where $a_0,b_0,c_0,d_0,a_1,b_1,c_1,d_1$ are functions of τ, χ, which are to be determined. From

$$T_\tau + TU = U^{[1]}T, \tag{A2}$$

and comparing the coefficients of $\xi^j (j = 3,2,1,0)$, yields

$$\begin{aligned}
&\xi^3 : b_1 = 0,\ c_1 = 0,\\
&\xi^2 : Ea_1 + 2ib_0 - E^{[1]}d_1 = 0,\ -F^{[1]}a_1 + Fd_1 - 2ic_0 = 0,\\
&\xi^1 : a_{1\tau} + \tfrac{1}{2}Fb_0 - \tfrac{1}{2}E^{[1]}c_0 = 0,\ d_{1\tau} + \tfrac{1}{2}Ec_0 - \tfrac{1}{2}F^{[1]}b_0 = 0,\\
&\qquad Ea_0 - E^{[1]}d_0 = 0,\ -F^{[1]}a_0 + Fd_0 = 0,\\
&\xi^0 : a_{0\tau} = b_{0\tau} = c_{0\tau} = d_{0\tau} = 0.
\end{aligned} \tag{A3}$$

Similarly, from

$$T_\chi + TV = V^{[1]}T, \tag{A4}$$

and comparing the coefficients of $\xi^j, j = 3,2,1,0$, we get

$$\begin{aligned}
&\xi^3 : \tfrac{1}{2}iR^{z[1]}a_1 - \tfrac{1}{2}iR^z a_1 + a_{1\chi} = 0,\ -\tfrac{1}{2}iR^{z[1]}d_1 + \tfrac{1}{2}iR^z d_1 + d_{1\chi} = 0,\\
&\xi^2 : a_{0\chi} + \tfrac{1}{2}iR^{z[1]}a_0 - \tfrac{1}{2}iR^{[z]}a_0 = 0,\ c_{0\chi} - \tfrac{1}{2}Sd_1 - \tfrac{1}{2}iR^z c_0 - \tfrac{1}{2}iR^{z[1]}c_0 + \tfrac{1}{2}S^{[1]}a_1 = 0,\\
&\qquad b_{0\chi} - \tfrac{1}{2}Ra_1 + \tfrac{1}{2}iR^z b_0 + \tfrac{1}{2}iR^{z[1]}b_0 + \tfrac{1}{2}R^{[1]}d_1 = 0,\ d_{0\chi} - \tfrac{1}{2}iR^{z[1]}d_0 + \tfrac{1}{2}iR^{[z]}d_0 = 0,\\
&\xi^1 : a_{1\chi} + \tfrac{1}{2}R^{[1]}c_0 - \tfrac{1}{2}Sb_0 = 0,\ d_{1\chi} + \tfrac{1}{2}S^{[1]}b_0 - \tfrac{1}{2}Rc_0 = 0,\\
&\qquad -Ra_0 + R^{[1]}d_0 = 0,\ S^{[1]}a_0 - Sd_0 = 0,\\
&\xi^0 : a_{0\chi} = b_{0\chi} = c_{0\chi} = d_{0\chi} = 0.
\end{aligned} \tag{A5}$$

In order to obtain nontrivial solutions, we shall construct a basic (or onefold) Darboux matrix T with $a_0 = 0$ and $d_0 = 0$. If we set $a_0 \neq 0$, then d_0 is not zero. Furthermore, we know that some coefficients (a_0,d_0) of T are constants, which generates trivial DT: $E^{[1]} = \frac{a_0}{d_0}E$ and $F^{[1]} = \frac{d_0}{a_0}F$.

APPENDIX B: DETERMINANT REPRESENTATION OF *n*-ORDER DARBOUX MATRIX, a_0, d_0, b_1, AND c_1

(1) For $n = 2k\ (k = 1,2,3,\ldots)$, the n-fold DT of the unreduced rotating RMB equations can be expressed as

$$T_n = T_n(\xi;\xi_1,\xi_2,\ldots,\xi_n) = \begin{pmatrix} \frac{\widetilde{(T_n)_{11}}}{W_n} & \frac{\widetilde{(T_n)_{12}}}{W_n} \\ \frac{\widetilde{(T_n)_{21}}}{\widetilde{W_n}} & \frac{\widetilde{(T_n)_{22}}}{\widetilde{W_n}} \end{pmatrix}, \tag{B1}$$

$$a_0 = \frac{\widetilde{W_n}}{W_n} = \frac{1}{d_0}, b_1 = \frac{\delta_{n1}}{W_n}, c_1 = \frac{\delta_{n2}}{\widetilde{W_n}} \tag{B2}$$

with

$$W_n = \begin{vmatrix}
\xi_1^{n-1}\psi_{11} & \xi_1^{n-2}\psi_{12} & \ldots & \xi_1\psi_{11} & \psi_{12}\\
\xi_2^{n-1}\psi_{21} & \xi_2^{n-2}\psi_{22} & \ldots & \xi_2\psi_{21} & \psi_{22}\\
\vdots & \vdots & \vdots & \vdots & \vdots\\
\xi_{n-1}^{n-1}\psi_{n-11} & \xi_{n-1}^{n-2}\psi_{n-12} & \ldots & \xi_{n-1}\psi_{n-11} & \psi_{n-12}\\
\xi_n^{n-1}\psi_{n1} & \xi_n^{n-2}\psi_{n2} & \ldots & \xi_n\psi_{n1} & \psi_{n2}
\end{vmatrix},$$

$$\widetilde{(T_n)_{11}} = \begin{vmatrix}
\xi^n & 0 & \ldots & \xi^2 & 0 & 1\\
\xi_1^n\psi_{11} & \xi_1^{n-1}\psi_{12} & \ldots & \xi_1^2\psi_{11} & \xi_1\psi_{12} & \psi_{11}\\
\xi_2^n\psi_{21} & \xi_2^{n-1}\psi_{22} & \ldots & \xi_2^2\psi_{21} & \xi_2\psi_{22} & \psi_{21}\\
\vdots & \vdots & \vdots & \vdots & \vdots & \vdots\\
\xi_{n-1}^n\psi_{n-11} & \xi_{n-1}^{n-1}\psi_{n-12} & \ldots & \xi_{n-1}^2\psi_{n-11} & \xi_{n-1}\psi_{n-12} & \psi_{n-11}\\
\xi_n^n\psi_{n1} & \xi_n^{n-1}\psi_{n2} & \ldots & \xi_n^2\psi_{n1} & \xi_n\psi_{n2} & \psi_{n1}
\end{vmatrix},$$

$$\widetilde{(T_n)_{12}} = \begin{vmatrix} 0 & \xi^n & \dots & 0 & \xi & 0 \\ \xi_1^n\psi_{11} & \xi_1^{n-1}\psi_{12} & \dots & \xi_1^2\psi_{11} & \xi_1\psi_{12} & \psi_{11} \\ \xi_2^n\psi_{21} & \xi_2^{n-1}\psi_{22} & \dots & \xi_2^2\psi_{21} & \xi_2\psi_{22} & \psi_{21} \\ \vdots & \vdots & \vdots & \vdots & \vdots & \vdots \\ \xi_{n-1}^n\psi_{n-11} & \xi_{n-1}^{n-1}\psi_{n-12} & \dots & \xi_{n-1}^2\psi_{n-11} & \xi_{n-1}\psi_{n-12} & \psi_{n-11} \\ \xi_n^n\psi_{n1} & \xi_n^{n-1}\psi_{n2} & \dots & \xi_n^2\psi_{n1} & \xi_n\psi_{n2} & \psi_{n1} \end{vmatrix},$$

$$\widetilde{W_n} = \begin{vmatrix} \xi_1^{n-1}\psi_{12} & \xi_1^{n-2}\psi_{11} & \dots & \xi_1\psi_{12} & \psi_{11} \\ \xi_2^{n-1}\psi_{22} & \xi_2^{n-2}\psi_{21} & \dots & \xi_2\psi_{22} & \psi_{21} \\ \vdots & \vdots & \vdots & \vdots & \vdots \\ \xi_{n-1}^{n-1}\psi_{n-12} & \xi_{n-1}^{n-2}\psi_{n-11} & \dots & \xi_{n-1}\psi_{n-12} & \psi_{n-11} \\ \xi_n^{n-1}\psi_{n2} & \xi_n^{n-2}\psi_{n1} & \dots & \xi_n\psi_{n2} & \psi_{n1} \end{vmatrix},$$

$$\widetilde{(T_n)_{21}} = \begin{vmatrix} 0 & \xi^n & \dots & 0 & \xi & 0 \\ \xi_1^n\psi_{12} & \xi_1^{n-1}\psi_{11} & \dots & \xi_1^2\psi_{12} & \xi_1\psi_{11} & \psi_{12} \\ \xi_2^n\psi_{22} & \xi_2^{n-1}\psi_{21} & \dots & \xi_2^2\psi_{22} & \xi_2\psi_{21} & \psi_{22} \\ \vdots & \vdots & \vdots & \vdots & \vdots & \vdots \\ \xi_{n-1}^n\psi_{n-12} & \xi_{n-1}^{n-1}\psi_{n-11} & \dots & \xi_{n-1}^2\psi_{n-12} & \xi_{n-1}\psi_{n-11} & \psi_{n-12} \\ \xi_n^n\psi_{n2} & \xi_n^{n-1}\psi_{n1} & \dots & \xi_n^2\psi_{n2} & \xi_n\psi_{n1} & \psi_{n2} \end{vmatrix},$$

$$\widetilde{(T_n)_{22}} = \begin{vmatrix} \xi^n & 0 & \dots & \xi^2 & 0 & 1 \\ \xi_1^n\psi_{12} & \xi_1^{n-1}\psi_{11} & \dots & \xi_1^2\psi_{12} & \xi_1\psi_{11} & \psi_{12} \\ \xi_2^n\psi_{22} & \xi_2^{n-1}\psi_{21} & \dots & \xi_2^2\psi_{22} & \xi_2\psi_{21} & \psi_{22} \\ \vdots & \vdots & \vdots & \vdots & \vdots & \vdots \\ \xi_{n-1}^n\psi_{n-12} & \xi_{n-1}^{n-1}\psi_{n-11} & \dots & \xi_{n-1}^2\psi_{n-12} & \xi_{n-1}\psi_{n-11} & \psi_{n-12} \\ \xi_n^n\psi_{n2} & \xi_n^{n-1}\psi_{n1} & \dots & \xi_n^2\psi_{n2} & \xi_n\psi_{n1} & \psi_{n2} \end{vmatrix},$$

$$\delta_{n1} = -\begin{vmatrix} \xi_1^n\psi_{11} & \xi_1^{n-2}\psi_{11} & \dots & \xi_1\psi_{12} & \psi_{11} \\ \xi_2^n\psi_{21} & \xi_2^{n-2}\psi_{21} & \dots & \xi_2\psi_{22} & \psi_{21} \\ \vdots & \vdots & \vdots & \vdots & \vdots \\ \xi_{n-1}^n\psi_{n-11} & \xi_{n-1}^{n-2}\psi_{n-11} & \dots & \xi_{n-1}\psi_{n-12} & \psi_{n-11} \\ \xi_n^n\psi_{n1} & \xi_n^{n-2}\psi_{n1} & \dots & \xi_n\psi_{n2} & \psi_{n1} \end{vmatrix},$$

$$\delta_{n2} = -\begin{vmatrix} \xi_1^n\psi_{12} & \xi_1^{n-2}\psi_{12} & \dots & \xi_1\psi_{11} & \psi_{12} \\ \xi_2^n\psi_{22} & \xi_2^{n-2}\psi_{22} & \dots & \xi_2\psi_{21} & \psi_{22} \\ \vdots & \vdots & \vdots & \vdots & \vdots \\ \xi_{n-1}^n\psi_{n-12} & \xi_{n-1}^{n-2}\psi_{n-12} & \dots & \xi_{n-1}\psi_{n-11} & \psi_{n-12} \\ \xi_n^n\psi_{n2} & \xi_n^{n-2}\psi_{n2} & \dots & \xi_n\psi_{n1} & \psi_{n2} \end{vmatrix}.$$

(2) For $n = 2k + 1 (k = 1,2,3, \cdots)$, then

$$T_n = T_n(\xi;\xi_1,\xi_2,\dots,\xi_n) = \begin{pmatrix} \frac{\widehat{(T_n)_{11}}}{Q_n} & \frac{\widehat{(T_n)_{12}}}{Q_n} \\ \frac{\widehat{(T_n)_{21}}}{\widehat{Q_n}} & \frac{\widehat{(T_n)_{22}}}{\widehat{Q_n}} \end{pmatrix}, \tag{B3}$$

$$a_0 = -\frac{\widehat{Q_n}}{Q_n} = \frac{1}{d_0}, b_1 = \frac{\delta_{n3}}{Q_n}, c_1 = \frac{\delta_{n4}}{\widehat{Q_n}} \tag{B4}$$

with

$$Q_n = \begin{vmatrix} \xi_1^{n-1}\psi_{11} & \xi_1^{n-2}\psi_{12} & \dots & \xi_1^2\psi_{11} & \xi_1\psi_{12} & \psi_{11} \\ \xi_2^{n-1}\psi_{21} & \xi_2^{n-2}\psi_{22} & \dots & \xi_2^2\psi_{21} & \xi_2\psi_{22} & \psi_{21} \\ \vdots & \vdots & \vdots & \vdots & \vdots & \vdots \\ \xi_n^{n-1}\psi_{n1} & \xi_n^{n-2}\psi_{n2} & \dots & \xi_n^2\psi_{n1} & \xi_n\psi_{n2} & \psi_{n1} \end{vmatrix},$$

$$\widehat{(T_n)_{11}} = \begin{vmatrix} \xi^n & 0 & \dots & \xi^3 & 0 & \xi & 0 \\ \xi_1^n\psi_{11} & \xi_1^{n-1}\psi_{12} & \dots & \xi_1^3\psi_{11} & \xi_1^2\psi_{12} & \xi_1\psi_{11} & -\psi_{12} \\ \xi_2^n\psi_{21} & \xi_2^{n-1}\psi_{22} & \dots & \xi_2^3\psi_{21} & \xi_2^2\psi_{22} & \xi_2\psi_{21} & -\psi_{22} \\ \vdots & \vdots & \vdots & \vdots & \vdots & \vdots & \vdots \\ \xi_n^n\psi_{n1} & \xi_n^{n-1}\psi_{n2} & \dots & \xi_n^3\psi_{n1} & \xi_n^2\psi_{n2} & \xi_n\psi_{n1} & -\psi_{n2} \end{vmatrix},$$

$$\widehat{(T_n)_{12}} = \begin{vmatrix} 0 & \xi^{n-1} & \dots & 0 & \xi^2 & 0 & -1 \\ \xi_1^n\psi_{11} & \xi_1^{n-1}\psi_{12} & \dots & \xi_1^3\psi_{11} & \xi_1^2\psi_{12} & \xi_1\psi_{11} & -\psi_{12} \\ \xi_2^n\psi_{21} & \xi_2^{n-1}\psi_{22} & \dots & \xi_2^3\psi_{21} & \xi_2^2\psi_{22} & \xi_2\psi_{21} & -\psi_{22} \\ \vdots & \vdots & \vdots & \vdots & \vdots & \vdots & \vdots \\ \xi_n^n\psi_{n1} & \xi_n^{n-1}\psi_{n2} & \dots & \xi_n^3\psi_{n1} & \xi_n^2\psi_{n2} & \xi_n\psi_{n1} & -\psi_{n2} \end{vmatrix},$$

$$\widehat{Q_n} = \begin{vmatrix} \xi_1^{n-1}\psi_{12} & \xi_1^{n-2}\psi_{11} & \dots & \xi_1^2\psi_{12} & \xi_1\psi_{11} & \psi_{12} \\ \xi_2^{n-1}\psi_{22} & \xi_2^{n-2}\psi_{21} & \dots & \xi_2^2\psi_{22} & \xi_2\psi_{21} & \psi_{22} \\ \vdots & \vdots & \vdots & \vdots & \vdots & \vdots \\ \xi_n^{n-1}\psi_{n2} & \xi_n^{n-2}\psi_{n1} & \dots & \xi_n^2\psi_{n2} & \xi_n\psi_{n1} & \psi_{n2} \end{vmatrix},$$

$$\widehat{(T_n)_{21}} = \begin{vmatrix} 0 & \xi^{n-1} & ... & 0 & \xi^2 & 0 & -1 \\ \xi_1^n\psi_{12} & \xi_1^{n-1}\psi_{11} & \dots & \xi_1^3\psi_{12} & \xi_1^2\psi_{11} & \xi_1\psi_{12} & -\psi_{11} \\ \xi_2^n\psi_{22} & \xi_2^{n-1}\psi_{21} & \dots & \xi_2^3\psi_{22} & \xi_2^2\psi_{21} & \xi_2\psi_{22} & -\psi_{21} \\ \vdots & \vdots & \vdots & \vdots & \vdots & \vdots & \vdots \\ \xi_n^n\psi_{n2} & \xi_n^{n-1}\psi_{n1} & \dots & \xi_n^3\psi_{n2} & \xi_n^2\psi_{n1} & \xi_n\psi_{n2} & -\psi_{n1} \end{vmatrix},$$

$$\widehat{(T_n)_{22}} = \begin{vmatrix} \xi^n & 0 & \dots & \xi^3 & 0 & \xi & 0 \\ \xi_1^n\psi_{12} & \xi_1^{n-1}\psi_{11} & \dots & \xi_1^3\psi_{12} & \xi_1^2\psi_{11} & \xi_1\psi_{12} & -\psi_{11} \\ \xi_2^n\psi_{22} & \xi_2^{n-1}\psi_{21} & \dots & \xi_2^3\psi_{22} & \xi_2^2\psi_{21} & \xi_2\psi_{22} & -\psi_{21} \\ \vdots & \vdots & \vdots & \vdots & \vdots & \vdots & \vdots \\ \xi_n^n\psi_{n2} & \xi_n^{n-1}\psi_{n1} & \dots & \xi_n^3\psi_{n2} & \xi_n^2\psi_{n1} & \xi_n\psi_{n2} & -\psi_{n1} \end{vmatrix},$$

$$\delta_{n3} = \begin{vmatrix} \xi_1^n\psi_{11} & \xi_1^{n-2}\psi_{11} & \dots & \xi_1^2\psi_{12} & \xi_1\psi_{11} & \psi_{12} \\ \xi_2^n\psi_{21} & \xi_2^{n-2}\psi_{21} & \dots & \xi_2^2\psi_{22} & \xi_2\psi_{21} & \psi_{22} \\ \vdots & \vdots & \vdots & \vdots & \vdots & \vdots \\ \xi_n^n\psi_{n1} & \xi_n^{n-2}\psi_{n1} & \dots & \xi_n^2\psi_{n2} & \xi_n\psi_{n1} & \psi_{n2} \end{vmatrix},$$

$$\delta_{n4} = \begin{vmatrix} \xi_1^n\psi_{12} & \xi_1^{n-2}\psi_{12} & \dots & \xi_1^2\psi_{11} & \xi_1\psi_{12} & \psi_{11} \\ \xi_2^n\psi_{22} & \xi_2^{n-2}\psi_{22} & \dots & \xi_2^2\psi_{21} & \xi_2\psi_{22} & \psi_{21} \\ \vdots & \vdots & \vdots & \vdots & \vdots & \vdots \\ \xi_n^n\psi_{n2} & \xi_n^{n-2}\psi_{n2} & \dots & \xi_n^2\psi_{n1} & \xi_n\psi_{n2} & \psi_{n1} \end{vmatrix}.$$

[1] T. Brabec and F. Krausz, Rev. Mod. Phys. **72**, 545 (2000).
[2] F. Krausz and M. Ivanov, Rev. Mod. Phys. **81**, 163 (2009).
[3] E. Goulielmakis, M. Schultze, M. Hofstetter, V. S. Yakovlev, J. Gagnon, M. Uiberacker, A. L. Aquila, E. M. Gullikson, D. T. Attwood, R. Kienberger, F. Krausz, and U. Kleineberg, Science **320**, 1614 (2008).
[4] G. Mourou and T. Tajima, Science **331**, 41 (2011).
[5] E. M. Belenov and A. V. Nazarkin, Pis'ma Zh. Eksp. Teor. Fiz. **51**, 252 (1990) [JETP Lett. **51**, 288 (1990)].
[6] J. E. Rothenberg, Opt. Lett. **17**, 1340 (1992).
[7] J. K. Ranka and A. L. Gaeta, Opt. Lett. **23**, 534 (1998).
[8] E. D. Farnum and J. Nathan Kutz, Opt. Lett. **35**, 3033 (2010).
[9] H. Leblond and D. Mihalache, Rom. Rep. Phys. **63**, 1254 (2011).
[10] H. Leblond and D. Mihalache, Phys. Rep. **523**, 61 (2013).
[11] S. V. Sazonov, Bull. Russ. Acad. Sci: Phys. **75**, 157 (2011).
[12] T. Brabec and F. Krausz, Phys. Rev. Lett. **78**, 3282 (1997).
[13] G. Genty, P. Kinsler, B. Kibler, and J. M. Dudley, Opt. Expr. **15**, 5382 (2007).
[14] A. I. Maimistov and M. Basharov, *Nonlinear Optical Waves* (Kluwer Academic Publishers, Dordrecht, 1999).
[15] M. Geissler, G. Tempea, A. Scrinzi, M. Schnurer, F. Krausz, and T. Brabec, Phys. Rev. Lett. **83**, 2930 (1999).
[16] M. Agrotis, N. M. Ercolani, S. A. Glasgow, and J. V. Moloney, Physica D. **138**, 134 (2000).
[17] A. I. Maimistov and J.-G. Caputo, Opti. Spectrosc. **94**, 245 (2003).
[18] T. Schäfer and C. E. Wayne, Physica D **196**, 90 (2004).
[19] S. Amiranashvili, A. G. Vladimirov, and U. Bandelow, Phys. Rev. A **77**, 063821 (2008).
[20] Sh. Amiranashvili, U. Bandelow, and N. Akhmediev, Phys. Rev. A **87**, 013805 (2013).
[21] A. V. Husakou and J. Herrmann, Phys. Rev. Lett. **87**, 203901 (2001).
[22] J. K. Eilbeck, J. D. Gibbon, P. J. Caudrey, and R. K. Bullough, J. Phys. A: Math. Nucl. Gen. **6**, 1337 (1973).
[23] P. J. Caudrey, J. C. Eilbeck, and J. D. Gibbon, J. Inst. Math. Appl. **14**, 375 (1974).
[24] R. K. Dodd, J. K. Eilbeck, and J. D. Gibbon, *Solitons and Nonlinear Wave Equations* (Academic Press, London, 1982).
[25] S. L. McCall and E. L. Hahn, Phys. Rev. Lett. **18**, 908 (1967).
[26] S. L. McHall and E. L. Hahn, Phys. Rev. **183**, 457 (1969).
[27] H. M. Gibbs and R. E. Slusher, Phys. Rev. A **6**, 2326 (1972).
[28] G. L. Lamb, Rev. Mod. Phys. **43**, 99 (1971).
[29] H. A. Haus, Rev. Mod. Phys. **51**, 331 (1979).
[30] R. K. Bullough, P. M. Jack, P. W. Kitchenside, and R. Saunders, Phys. Scr. Scripta. **20**, 364 (1979).
[31] A. I. Maimistov, A. M. Basharov, S. O. Elyutin, and Yu. M. Sklyarov, Phys. Rep. **191**, 1 (1990).
[32] A. I. Maimistov, Quantum. Electron. **30**, 287 (2000).
[33] A. A. Zabolotskii, Eur. Phys. J. Spec. Top. **173**, 193 (2009).
[34] A. I. Maimistov, Quantum. Electron. **40**, 756 (2010).
[35] H. Steudel and A. A. Zabolotskii, J. Phys. A: Math. Gen. **37**, 5047 (2004).
[36] D. J. Kaup and A. C. Newell, J. Math. Phys. **19**, 798 (1978).
[37] H. Steudel, A. A. Zabolotskii, and R. Meinel, Phys. Rev. E **72**, 056608 (2005).
[38] A. A. Zabolotskii, Phys. Rev. E **75**, 036612 (2007).
[39] A. A. Zabolotskii, Physica D **237**, 540 (2008).
[40] J. He, S. Xu, and K. Porsezian, Phys. Rev. E **86**, 066603 (2012).
[41] C. Li, J. He, and K. Porsezian, Phys. Rev. E **87**, 012913 (2013).
[42] C. Kharif, E. Pelinovsky, and A. Slunyaev, *Rogue Waves in the Ocean* (Springer, Berlin, 2009).
[43] A. Chabchoub, N. P. Hoffmann, and N. Akhmediev, Phys. Rev. Lett. **106**, 204502 (2011).
[44] A. Chabchoub, N. Hoffmann, M. Onorato, and N. Akhmediev, Phys. Rev. X **2**, 011015 (2012).
[45] D. R. Solli, C. Ropers, P. Koonath, and B. Jalali, Nature **450**, 1054 (2007).
[46] B. Kibler, J. Fatome, C. Finot, G. Millot, F. Dias, G. Genty, N. Akhmediev, and J. M. Dudley, Nat. Phys. **6**, 790 (2010).
[47] D. H. Peregrine, J. Aust. Math. Soc. Series B, Appl. Math. **25**, 16 (1983).
[48] V. B. Matveev and M. A. Salle, *Darboux Transfromations and Solitons* (Springer-Verlag, Berlin, 1991).
[49] J. S. He, L. Zhang, Y. Cheng, and Y. S. Li, Sci. China A: Math. **49**, 1867 (2006).
[50] K. Imai, J. Phys. Soc. Jpn. **68**, 355 (1999).
[51] H. Steudel, J. Phys. A: Math. Gen. **36**, 1931 (2003).
[52] P. Dubard and V. B. Matveev, Nat. Hazards. Earth. Syst. Sci. **11**, 667 (2011).
[53] Y. Ohta and J. K. Yang, Proc. R. Soc. A. **468**, 1716 (2012).
[54] D. J. Kedziora, A. Ankiewicz, and N. Akhmediev, Phys. Rev. E **84**, 056611 (2011).
[55] B. Guo, L. Ling, and Q. P. Liu, Phys. Rev. E **85**, 026607 (2012).
[56] P. Gaillard, J. Math. Phys. **54**, 013504 (2013).
[57] J. S. He, H. R. Zhang, L. H. Wang, K. Porsezian, and A. S. Fokas, Phys. Rev. E **87**, 052914 (2013).
[58] S. W. Xu, J. S. He, and L. H. Wang, J. Phys. A: Math. Theor. **44**, 305203 (2011).
[59] S. W. Xu and J. S. He, J. Math. Phys. **53**, 063507 (2012).